J. Fluid Mech. (2001), *vol.* 446, *pp.* 133–171.
DOI: 10.1017/S0022112001005742 Printed in the United Kingdom

Quasi-modes in boundary-layer-type flows. Part 1. Inviscid two-dimensional spatially harmonic perturbations

By VICTOR I. SHRIRA† AND IGOR A. SAZONOV

Department of Applied Mathematics, University College Cork, Cork, Ireland
e-mail: v.i.shrira@keele.ac.uk; i.sazonov@ucc.ie

(Received 6 June 2000 and in revised form 18 May 2001)

The work, being the first in a series concerned with the evolution of small perturbations in shear flows, studies the linear initial-value problem for inviscid spatially harmonic perturbations of two-dimensional shear flows of boundary-layer type without inflection points. Of main interest are the perturbations of wavelengths $2\pi/k$ long compared to the boundary-layer thickness H, $kH = \epsilon \ll 1$. By means of an asymptotic expansion, based on the smallness of ϵ, we show that for a generic initial perturbation there is a long time interval of duration $\sim \epsilon^{-3}\ln(1/\epsilon)$, where the perturbation representing an aggregate of continuous spectrum modes of the Rayleigh equation behaves as if it were a single discrete spectrum mode having no singularity to the leading order. Following Briggs *et al.* (1970), who introduced the concept of decaying wave-like perturbations due to the presence of the 'Landau pole' into hydrodynamics, we call this object a *quasi-mode*. We trace analytically how the quasi-mode contribution to the entire perturbation field evolves for different field characteristics. We find that over $O(\epsilon^{-3}\ln(1/\epsilon))$ time interval, the quasi-mode dominates the velocity field. In particular, over this interval the share of the perturbation energy contained in the quasi-mode is very close to 1, with the discrepancy in the generic case being $O(\epsilon^4)$ ($O(\epsilon^6)$ for the Blasius flow). The mode is weakly decaying, as $\exp(-\epsilon^3 t)$. At larger times the quasi-mode ceases to dominate in the perturbation field and the perturbation decay law switches to the classical t^{-2}. By definition, the quasi-modes are singular in a critical layer; however, we show that in our context their singularity does not appear in the leading order. From the physical viewpoint, the presence of a small jump in the higher orders has little significance to the manner in which perturbations of the flow can participate in linear and nonlinear resonant interactions. Since we have established that the decay rate of the quasi-modes sharply increases with the increase of the wavenumber, one of the major conjectures of the analysis is that the long-wave components prevail in the large-time asymptotics of a wide class of initial perturbations, not necessarily the predominantly long-wave perturbations. Thus, the explicit expressions derived in the long-wave approximation describe the asymptotics of a much wider class of initial conditions than might have been anticipated. The concept of quasi-modes also enables us to shed new light on the foundations of the method of piecewise linear approximations widely used in hydrodynamics.

† Present address: Department of Mathematics, Keele University, Keele, ST5 5BG, UK.

1. Introduction

Dynamics of small perturbations in shear flows belongs to one of the classical and the most studied subjects in fluid mechanics. Indeed, there is an impressive list of achievements summarized in numerous monographs and textbooks (e.g. Lin 1955; Chandrasekhar 1981; Drazin & Reid 1981; Craik 1985; Schmidt & Henningson 2001). However, even for the simplest plane parallel flows of uniform inviscid fluid, there are still important open questions which have not so far received the attention they merit. Evolution of infinitesimal perturbations in shear flows can always be naturally described in terms of wavelike normal modes (e.g. Lin 1955; Drazin & Reid 1981) and attention has been focused mainly upon the search for and analysis of linearly unstable eigen modes. The existence of such modes in the case of plane parallel shear flows of homogeneous fluid is determined by the famous Rayleigh theorem which requires for instability the presence of inflection points in the basic flow profile. When linearly unstable modes exist, they eventually prevail in the solution of linear and nonlinear initial problems, whatever the initial conditions. The situation is much less obvious when there are no linearly unstable modes. Remaining within the framework of the normal mode paradigm, strictly speaking, we should deal with a continuum of modes of continuous spectrum. The eigenmodes of the continuous spectrum, sometimes called Van Kampen–Case waves, are singular, exhibiting a logarithmic and pole-like singularity (e.g. Drazin & Reid 1981; Craik 1985; Kelbert & Sazonov 1996). Since, on the one hand, it has been established that any initial perturbation composed of such modes decays at large times as t^{-2} (Case 1960; Dickey 1960; Maslowe 1981) and, on the other hand, owing to the formidable technical difficulties in analysing evolutionary problems in terms of such singular modes, there has been little progress for shear flows without inflection points in the general problem setting.

In parallel, an initially very remote line of research was initiated by the classical work by Landau (1946), where it was shown how interaction of an electromagnetic wave and particles can result in wave damping or amplification. In our context, the important point is that the damped waves can be described as the contribution to a pole (the Landau pole) lying on a appropriately defined Riemann surface. The concept of the so-called Landau damping became so widely used in plasma physics that referencing to the original work soon almost disappeared there. The concept penetrated into hydrodynamics as well, the first crucial step in this context was made by Briggs, Daugherty & Levy (1970). Investigating a particular problem concerned with cross-field electron beams which proves to be mathematically equivalent to the Rayleigh equation for rotating inviscid shear flows, they found what happens to a discrete spectrum mode solution corresponding to a rotating basic shear flow with a break, if the break is slightly smoothed. Although the work was addressing a specific hydrodynamic problem, the conceptual importance of the results goes far beyond it. Briggs *et al.* (1970) seem to be the first to reveal deep mathematical similarity between the wave–particle interaction and the wave–fluid interaction with the waves of continuous spectrum playing the role of the particles. They demonstrated how to find the pole-like singularities similar to the 'Landau pole' by appropriate analytical continuation and described the essence of the specific wave-like motions due to the pole contribution. These motions, for which the term *quasi-modes* was coined, being distinct from the 'true' eigenmodes represent an aggregate of the continuous spectrum modes and manifest themselves as decaying waves characterized by jumps in the velocity. It was suggested that the quasi-modes with a small decay rate can be destabilized by an external perturbation and thus turn into growing true modes. It was conjectured that even the decaying quasi-modes ought to be an intermediate asymptotics of the generic initial problem under certain (unspecified) circumstances. Much later, it was confirmed experimentally and by numerical simulation that, at least for particular model profiles, the quasi-mode indeed represents the intermediate asymptotics of the initial problem (Schecter *et al.* 2000). Balmforth *et al.* (1997) successfully used quasi-modes to describe evolution of the vorticity defects in a uniform shear flow, but overall, in our opinion, the concept of quasi-modes in hydrodynamics has not received the attention it merits and its full potential has not been realized. The concept has been successfully applied only to a limited number of specific cases, mostly corresponding to the situations of somewhat smoothed breaks in the basic flow (Briggs *et al.* 1970; Mironov & Sazonov 1989; Schecter *et al.* 2000). Among the reasons preventing, in our view, a wider use of the quasi-mode concept we mention a few: first, any important classes of flows where the quasi-modes appear naturally in the generic situation have not been identified; secondly, no analytical study describing all stages of the perturbation evolution† and, in particular, quantifying the quasi-mode dominance, have been ever carried out; thirdly, the presence of jumps is one of the most unpleasant features of the quasi-modes, and pointing out the situations of interest where the jumps can be neglected would have been of great help. The present work fills this gap: first, we show, that for a particular very important class of shear flows without inflection points, namely, for the boundary-layer-type flows, the quasi-modes represent the most natural way of describing the perturbation evolution on certain time scales, secondly, we quantify the dominance of the quasi-mode in different fields, and trace analytically and numerically the entire picture of the field evolution; thirdly, we show that for the boundary layers the quasi-mode jumps are very small and we explain when and why the jumps can be neglected.

The study of perturbation evolution in boundary-layer-type flows has a rich history. The problem was revisited in a different context and considerable progress was achieved by means of the so-called triple-deck scheme (e.g. Smith 1982). For perturbations long compared to the boundary-layer thickness, weakly nonlinear solutions to the Navier–Stokes equations were derived in terms of an asymptotic expansion in powers of the natural small parameter ϵ characterizing smallness of the layer thickness compared to a typical wavelength. To the leading order, the solution proves to be inviscid. In our context, the central point is that at certain timescales arbitrary long-wave perturbations behave as if they were a single discrete mode having no singularities to the leading order, whereas, in fact, they represent an aggregate of the singular modes of continuous spectrum (Shrira 1989). Although in Shrira (1989) this fact was attributed correctly to the quasi-mode manifestation and a rough estimate of the quasi-mode lifespan was given, the main thrust in this and later works in this vein was on exploitation of the fact rather than its exploration. Such wavelike motions were encountered in many different situations and sometimes were called 'vorticity waves', since the 'restoring force' is due to the basic flow vorticity gradient (e.g. Pedley & Stephanoff 1985; Shrira & Voronovich 1996; Voronovich, Shrira & Stepanyants 1998*a*). Although works based upon the triple-deck scheme alone are numbered in hundreds, in our opinion, the essence of the underlying asympotics has not been fully clarified. One of the main aims of this work is to clarify the mathematical foundations of the widely used approach from the quasi-mode perspective.

We also address another outstanding classical problem, that of piecewise linear approximations in fluid mechanics. The issue of when, why and in what sense the

† The papers by Mironov & Sazonov (1989) and Balmforth *et al.* (1997) were confined to some special flows.

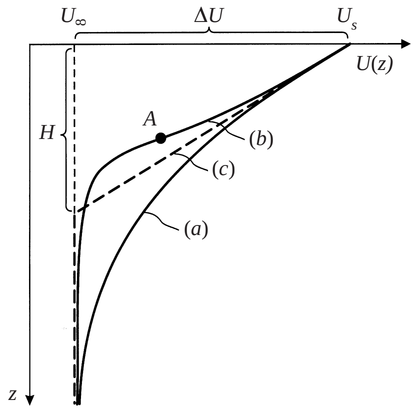

FIGURE 1. Boundary-layer-type flows without (*a*) and with (*b*) inflection point A. Piecewise linear approximation (*c*).

piecewise linear models work has never been properly addressed to our knowledge. Although there exists a clear understanding of what happens if a single break (see figure 1) is slightly smoothed (Briggs *et al.* 1970; Mironov & Sazonov 1989; Kelbert & Sazonov 1996; Schecter *et al.* 2000), the issue of approximation of a given smooth flow by a piecewise model remains much more an art than an algorithm-based technicality. There are no answers to the simplest questions of the type: How many breaks should be taken? What accuracy will be achieved and what qualitative features are lost? One of our aims is to obtain an insight into this problem by applying the quasi-mode concept.

The work is organized as follows. The present paper, which is the first part in the series, is concerned with the detailed analysis of the evolution of spatially harmonic initial perturbations to a boundary-layer-type shear flow. In § 2, starting with the standard governing equations, we formulate the basic initial-value problem, that of the evolution of longitudinally monochromatic perturbations with an arbitrary smooth initial vertical distribution. Here we introduce a Green's function of the problem and reformulate the problem in terms of this function. In § 3, we present the asymptotics of the Green's function for long-wave perturbations and then thoroughly investigate its singularities, in particular the Landau pole. In § 4, we study the contribution of all the singularities to the large-time asymptotics and show that the contribution due to this pole is, indeed, dominant over a long time interval, thus determining the intermediate asymptotics of the problem. In § 5, employing numerics, we investigate what happens beyond the range of applicability of the derived analytical asymptotics. The concluding § 6, contains a summary and a brief discussion of some implications of the quasi-mode concept, with attention being given to the problem of piecewise-linear approximations in hydrodynamics as illuminated by the concept.

Evolution of three-dimensional and non-monochromatic perturbations, including wave packets and broadband spectra, the effect of small viscosity, and relations between the inviscid and viscous results constitute the subject of the next parts of the work.

2. The initial-value problem for inviscid boundary-layer-type shear flows: statement of the problem

2.1. *Basic flow*

Consider a steady plane parallel flow of inviscid uniform fluid. We choose a Cartesian frame in which x, y and z are the downstream, spanwise and vertical coordinates, respectively. The flow being specified by its velocity profile $U(z)$ occupies the half-space $z > 0$. The vorticity of such a basic flow has only a y-component and equals $\Omega(z) = -U'(z)$ where hereinafter $(\ldots)'$ means differentiation with respect to z. For the typical boundary-layer-type flows, the functions $U(z)$ and $\Omega(z)$ vary monotonically, and

$$U(z \to \infty) \to U_\infty, \quad \Omega(z \to \infty) \to 0.$$

As a characteristic velocity scale for the basic flow, it is natural to take the total velocity variation $\Delta U = |U_s - U_\infty|$, i.e. the difference between the velocity at the surface U_s (hereinafter we use the subscript s to indicate that the variable is taken at the surface $z = 0$) and its value at infinity. We do not specify the values U_s and U_∞, since the convention differs for boundary layers of different types. Say, for the boundary layers over plate it is usually assumed that $U_\infty > 0$, $U_s = 0$ (then $\Delta U = U_\infty$, $U' > 0$), whereas for the free surface currents the convention is opposite: $U_\infty = 0$, $U_s > 0$ (then $\Delta U = U_s$, $U' < 0$).

Let us define a characteristic flow thickness H, as

$$H = \left| \frac{\int_0^\infty \Omega(z)\,\mathrm{d}z}{\Omega_s} \right| \equiv \frac{\Delta U}{|U_s'|}. \tag{2.1}$$

We assume that the flow profile is smooth enough in the sense that all its derivatives can be roughly estimated as follows

$$|U^{(n)}(z)| \lesssim \frac{\Delta U}{H^n}, \quad (n = 1, 2, \ldots). \tag{2.2}$$

2.2. *Governing equations*

Confining our attention in this first part of the work to consideration of two-dimensional small perturbations to the basic flow, let $u(z, x, t)$ and $w(z, x, t)$ be the horizontal and vertical velocity disturbances, respectively. It is convenient to introduce a stream function $\psi(z, x, t)$, such that: $u = -\partial_z \psi$ and $w = \partial_x \psi$. We assume the velocity disturbances to be small compared to ΔU, then w and ψ obey the linearized equation deduced from the Euler and continuity equations (e.g. Drazin & Reid 1981)

$$(\partial_t + U\partial_x)(\partial_z^2 + \partial_x^2)\psi - U''\partial_x\psi = 0. \tag{2.3}$$

Since the equation is longitudinally uniform it is convenient to apply the Fourier transform and consider the harmonic disturbances of the type: $\psi = \psi(z, t)\exp(\mathrm{i}kx)$, where k is the horizontal wavenumber. We can assume $k > 0$ without loss of generality. For such spatially harmonic disturbances the equation (2.3) takes the form

$$(\partial_t + \mathrm{i}kU)(\partial_z^2 - k^2)\psi - \mathrm{i}kU''\psi = 0. \tag{2.4a}$$

2.3. *Boundary and initial conditions*

We assume the 'no-flux' condition at the surface, i.e. $w(z=0) = 0$. The disturbances are also required to decay far from the surface, i.e. $u, w \to 0$ as $z \to \infty$. This implies that each of the spatial harmonics of the disturbance tend to $\exp(-kx)$ since the basic flow tends to a constant as $z \to \infty$. Thus, the boundary conditions in terms of stream function take the form:

$$\psi = 0 \quad \text{as} \quad z = 0, \tag{2.4b}$$

$$\partial_z\psi + k\psi \to 0 \quad \text{as} \quad z \to \infty. \tag{2.4c}$$

At the initial moment of time $t = 0$, the velocity field is assumed to be given:

$$\psi(t = 0) = \psi_0, \tag{2.4d}$$

where ψ_0 satisfies the boundary conditions (2.4b, c).

We consider generic initial conditions assuming the initial disturbances to be localized in the layer $z \lesssim H$ and decaying fast enough as z increases, with the vertical scale of the same order as that of the basic flow. We also assume non-vanishing of the integral over z of initial vorticity ω_0,

$$\omega_0 = (\partial_z^2 - k^2)\psi_0. \tag{2.5}$$

The above constraints are formalized as follows:

$$\omega_0/\Omega \rightarrow 0 \quad \text{as} \quad z \rightarrow \infty, \tag{2.6a}$$

$$|\partial_z^n \omega_0| \lesssim |\omega_0|/H^n \quad (n = 1, 2, \ldots), \tag{2.6b}$$

$$\int_0^\infty \omega_0(z)\,\mathrm{d}z \neq 0. \tag{2.6c}$$

The set of equations (2.4) under constraints (2.6) prescribes the initial-value problem which is the subject of our study.

2.4. *The Green's function*

We will study the evolution of perturbations specified by the initial-value problem (2.4) by employing Green's functions. Considering a problem where the disturbances have been suddenly excited at time $t = 0$ by an external force, we obtain an equation with a right-hand side

$$(\partial_t + \mathrm{i}kU)(\partial_z^2 - k^2)\psi - \mathrm{i}kU''\psi = \omega_0\delta(t), \tag{2.7}$$

where the stream function ψ now satisfies the causality principle: $\psi(t < 0) \equiv 0$ (i.e. there is no disturbance until the external force acts). For $t > 0$, the solution of the problem (2.7) and (2.4b, c) coincides with that of the initial problem we are looking for.

The solution for any initial disturbance can be presented in the integral form

$$\psi(z, k, t) = \int_0^\infty G(z \mid h; t)\,\omega_0(h)\,\mathrm{d}h, \tag{2.8}$$

where the kernel G is the Green's function specified by the equation

$$(\partial_t + \mathrm{i}kU)(\partial_z^2 - k^2)G - \mathrm{i}kU''G = \delta(z - h)\delta(t), \tag{2.9}$$

complemented by the boundary conditions (2.4b)–(2.4c), and the causality principle $G(t < 0) \equiv 0$.

2.5. *The Laplace transform*

To study the time dependence of the Green's function we apply the Laplace transform with respect to time

$$\tilde{G}(z \mid h; c) = \int_0^\infty G(z \mid h; t)\mathrm{e}^{-st}\,\mathrm{d}t. \tag{2.10}$$

We use the value $s = -\mathrm{i}kc$ as the Laplace transform parameter, where c can be interpreted as the complex phase velocity of spatially harmonic perturbation with wavenumber k. Then the inverse Laplace transform takes the form

$$G(z\,|\,h;t) = \frac{k}{2\pi}\int_{\Gamma} \tilde{G}(z\,|\,h;c)\mathrm{e}^{-\mathrm{i}kct}\,\mathrm{d}c, \tag{2.11}$$

where the integration contour Γ goes along the $\mathrm{Re}\,c$ axis above all singularities of $\tilde{G}(c)$.

Substituting (2.10) into (2.9) and dividing it by $\mathrm{i}k(-c+U)$, we obtain

$$(\partial_z^2 - k^2)\tilde{G} - \frac{U''}{U-c}\tilde{G} = \frac{\delta(z-h)}{\mathrm{i}k(U_h - c)}, \tag{2.12}$$

where $U_h = U(h)$.

Thus, we have reformulated the original boundary-value problem (2.4) into an equivalent one in terms of $\tilde{G}$: equation (2.12) with the boundary conditions (2.4b,c). The left-hand side of (2.12) is the famous Rayleigh equation for small harmonic (with respect to x and t) disturbances propagating with phase velocity c.

3. Singularities of the Green's function

To be able to describe eventually the evolution of arbitrary initial perturbations at large times, we first find an approximate explicit expression for the Green's function in the long-wave approximation which, as we justify *a posteriori* proves to be in a sense sufficient for arbitrary perturbations, then focus upon the singularities of the Green's function which determine the large-time asymptotics.

3.1. *Longwave asymptotics of the Green's function*

As we show below, the long-wave asymptotics is sufficient to describe the main features of boundary-layer dynamics. Hence, we seek a solution to the boundary-value problem (2.12) and (2.4b,c) employing the assumed smallness

$$\epsilon = kH \ll 1,$$

as a series in powers of ϵ.

The derivation of an asymptotic solution to this problem is far from being trivial, because a long-wave expansion cannot be applied directly to the Rayleigh equation for semi-infinite flows, as the term k^2 necessarily dominates over the term $U''/(U-c)$ when $z \to \infty$, and this is the principal difficulty of analysing the boundary-layer-type flows. Such a difficulty does not appear in the context of, say, channel flows, where a long-wave expansion is quite straightforward (Heisenberg 1924; Drazin & Reid 1981). Our derivation is based on the two different asymptotic expansions for partial solutions of the Rayleigh equation, which allows us to deal with an arbitrary smooth velocity profile. (The method applied by Kelbert & Sazonov 1996 for a similar problem required the flows to be constant beyond a layer of finite width.)

However, since for the main line of our study the specific way the Green's function is obtained is not vital, although being of interest in itself, we formulate here only the result we need, while the derivation is given in Appendix A. The leading terms of the expansion of $\tilde{G}$ sufficient for the further analysis can be presented as

$$\mathrm{i}k\tilde{G} = -V_z\, I_{\min\{z,h\}} + k\, V_\infty^2 \frac{V_z I_z\, I_h}{1 + k\, V_\infty^2 I_B}. \tag{3.1}$$

Here $I_Z = \int_0^Z V_z^{-2}\,\mathrm{d}z$ where Z stands for $z, h, B, \min\{z,h\}$, $V_Z = U_Z - c$; $U_Z \equiv U(Z)$, (here the subscript Z stands for the argument which might take the values z, h and

∞); B is a constant of the order of H which later drops out of the final expressions but is used in our intermediate manipulations.

Since the evolution of arbitrary initial perturbations at large times is determined by the singularities of the Green's function $\tilde{G}(c)$ analytically continued from the integration contour Γ over the entire complex c-plane, our main task at this stage is to continue analytically $\tilde{G}(c)$ and thoroughly study all its singularities: branch points and poles.

3.2. *Singularities of integral I_Z*

We first examine analytical continuation and singularities of the auxiliary function $I_Z(c)$ which enters into the derived expression for the Green's function (3.1). As a function of complex c it is specified by the integral

$$I_Z(c) = \int_0^Z \frac{\mathrm{d}z}{(U_z - c)^2}. \tag{3.2}$$

This function is uniquely defined on the Riemann surface with the cut $[U_s, U_Z]$ since the integrand does not contain any singularities on this surface. For our purposes, however, we have to continue $I_Z(c)$ through the cut.

Let $U_z \equiv U(z)$ admit an analytical continuation in the complex z-plane and be regular in the vicinity of the segment $[0, Z]$. Note, that any boundary-layer-type profile can be approximated by such functions. If we want to consider an analytical continuation of $I_Z(c)$ through the cut $[U_s, U_Z]$ and keep the analytical branch of $I_Z(c)$ we have to integrate along a contour passing around the point z_c in the complex z-plane. The point $z_c = U^{-1}(c)$ is the image of the point c; it is real when $c \in (U_s, U_Z)$. Thus, to obtain an analytical continuation under the cut we must use an integration contour at least partly lying on the complex z-plane.

Now we can proceed with an examination of the singularities of $I_Z(c)$. On changing the integration variable ($z \to U$) and adding and subtracting the term

$$z''(c) \int_{U_s}^{U_Z} \frac{\mathrm{d}U}{V_z}$$

the integral can be presented in the form

$$I_Z = \frac{1}{U_s' V_s} - \frac{1}{U_Z' V_Z} + \frac{U_c''}{U_c'} \log \frac{V_s}{V_Z} + J_Z, \tag{3.3a}$$

$$J_Z = \int_0^Z \left(\frac{U_c''}{(U_c')^3} - \frac{U_z''}{(U_z')^3} \right) \frac{U_z' \,\mathrm{d}z}{V_z}. \tag{3.3b}$$

Here, $U_c' = U'(z_c)$, $U_c'' = U''(z_c)$ $(U(z_c) = c)$; J_Z is an analytic function in the neighbourhood of the segment $[U_s, U_Z]$ if $U_z''(U_z')^{-3}$ is an analytical function in the vicinity of $[0, Z]$. Thus, we split the integral under consideration (3.2) into an explicit singular part and an implicit regular one, i.e. we 'pulled out' the singularities from the integral.

Hence, it easy to see from (3.3), that the singularities of integral $I_Z(c)$ are at the points $c = U_s$ and $c = U_Z$ and are simultaneously poles and logarithmic branch points.

The rule for choosing the proper branches is as follows: if c is real and $c \notin [U_s, U_Z]$, then $V_s/V_Z > 0$ and we take the real branch of $\log(V_s/V_Z)$; if c is real and $c \in [U_s, U_Z]$, then $V_s/V_Z < 0$ and we can show that

$$\log \frac{V_s}{V_Z} = \log\left(-\frac{V_s}{V_Z}\right) + \pi \mathrm{i}\,\mathrm{sgn}\, U_z', \quad c \in [U_s, U_Z], \tag{3.4}$$

where the real branch of $\log(-V_s/V_Z)$ is taken.

3.3. *The Landau pole*

Returning to the analysis of the Green's function (3.1) we can expect singularities in the integration limits of the integrals I_z, I_h and I_B. We discuss these singularities later, whereas now we focus upon the strongest singularity: the Landau pole. The pole is the singularity of most interest. Now we show that, even if there are no inflection points in the flow profile, the Green's function for the boundary-layer-type flows necessarily has a pole, characterized by, we stress this, an asymptotically small imaginary part.

Equating the denominator of the Green's function to zero, consider the roots of the equation

$$1 + k\int_0^B \frac{V_\infty^2}{V_z^2}\,\mathrm{d}z + O(k^2) = 0. \tag{3.5}$$

Using (3.3) and (3.4) we can present it in the form

$$1 + kV_\infty^2\left(\frac{1}{V_sU_s'} + \frac{U_c''}{(U_c')^3}\left[\log\left(-\frac{V_s}{V_B}\right) - \pi\mathrm{i}\right] - \frac{1}{V_BU_B'} + J_B\right) = 0, \tag{3.6}$$

where the logarithmic function is real when c is real and $c \in [U_s, U_B]$. Remembering that $V_s \equiv U_s - c$, $V_\infty \equiv U_\infty - c$ we can rewrite (3.6) in the form

$$\frac{1}{U_s - c}\left\{(U_s - c) + k\frac{(U_\infty - c)^2}{U_s'} - k(U_s - c)\frac{(U_\infty - c)^2 U_c''}{(U_c')^3}\pi\mathrm{i} + k(\ldots)\right\} = 0. \tag{3.7}$$

Dots denote the terms which contribute to higher orders in the expansion with respect to small k. From (3.7), we can easily see that $c \to U_s$ when $k \to 0$, and the case $k = 0$ is degenerate.

Solving the numerator of (3.7) by the successive iterations ($c - U_s = k(\ldots) + \text{h.o.t.}$) separately for the real and imaginary parts of the c_p, we find the leading terms for the pole:

$$c_p = c_r + \mathrm{i}c_i, \tag{3.8a}$$

$$c_r = U_s + k\frac{\Delta U^2}{U_s'} + O(k^2 \log k), \tag{3.8b}$$

$$c_i = \mathrm{sgn}(U_s')\,k^2\pi\,\frac{U_r''\,\Delta U^4}{(U_s')^4} + O(k^3\log k), \tag{3.8c}$$

where

$$U_r'' = \begin{cases} U_s'', & U_s'' \neq 0, \\ kU_s'''\dfrac{\Delta U^2}{U_s'^2}, & U_s'' = 0, \end{cases}$$

The subscript r in U_r'' means that we can take U_s'' for flows where $U_s'' \neq 0$, i.e. in the generic case. If, however, the flow is degenerate and $U_s'' = 0$, (e.g. the Blasius profile) we find the critical layer approximately from the equation (for certainty we distinguish critical layers occurring for real z_r and complex z_c: $U(z_r) = \mathrm{Re}\, c_p$,

$U(z_c) = c_p$. Obviously, $z_c = z_r + O(k^2)$)

$$U_s + U_s' z_r = c_r \quad \Rightarrow \quad z_r = k\frac{\Delta U^2}{U_s'^2} + O(k^2 \log k),$$

and then present the second derivative as

$$U_r'' \simeq U_s''' z_r \simeq k U_s''' \frac{\Delta U^2}{U_s'^2}.$$

In this case, the imaginary part of the phase velocity is $O(k^3)$ (It is easy to check that there is no need for higher orders in k in the expansion of the Wronskian (A 14) to find the leading term of c_i although c_i is of higher order itself):

$$c_i = \operatorname{sgn} U_s' k^3 \pi U_s''' \left(\frac{\Delta U}{U_s'}\right)^6 + O(k^4 \log k).$$

Even more degenerate flows in which $U_s''', U_s'''' = 0$, etc., can be considered similarly. The corresponding c_i will be of higher order with respect to k, but, so far, we are not aware of the existence of real flows justifying such an exercise.

Thus, we see that in a generic boundary layer the sign of the imaginary part of the pole c_p is determined by the value $U_s' U_s''$. In a flow without inflection points (figure 1, curve *a*), the product $U_z' U_z''$ is negative for all finite z including the surface. Therefore, $c_i < 0$ in such the flows, that is, the pole is always located in the lower half-plane, and should correspond to a decaying mode.

On the contrary, if $U_s' U_s'' > 0$, then the pole c_p is situated in the upper half-plane and corresponds to an unstable mode in the sense that the residue in it yields a solution with a growing factor $\exp[ik(x - c_r t) + kc_i t]$. Thus, $U_s' U_s'' > 0$ is a sufficient condition of instability for the flows under consideration.

Note that the condition necessarily implies the existence at least one inflection point (figure 1, curve *b*). Indeed, if U_z' is monotonic (as was assumed in § 2.1) then $U_z' U_z'' < 0$ for sufficiently large z for any boundary-layer-type flow. Then U_z'' should change its sign an odd number of times (at least one). If there is an even number of inflection points or if they are absent, then $U_s' U_s'' < 0$ and $c_i < 0$ for the found pole. (If we do not require monotonic behaviour of U_z' then $U_z' U_z''|_{z\to\infty} > 0$ becomes possible and $U_s' U_s'' > 0$ can be valid for an even number of inflection points, and the opposite inequality for an odd number.)

For the boundary layers without inflection points of the type (figure 1, curve *a*) that we are mostly interested in, where the existence of true discrete modes is strictly prohibited by the Rayleigh theorem, we have shown that there always exists a pole of the Green's function asymptotically close to the real axis. It is this smallness of the imaginary coordinate of the pole that, as we show later, makes the pole contribution dynamically significant.

From the general viewpoint, the nature of this pole is the same as that of the pole introduced by Landau (1946) in plasmas and by Briggs *et al.* (1970) in hydrodynamics. However, a brief comment regarding the pole position on the Riemann sheet (see figure 2) might be helpful.

It is more convenient to consider first the flows with an inflection point (see figure 1, curve *b*), where the pole c_p is in the upper half-plane. Denote by P_0 a sheet of complex c-plane with a cut $[U_{\min}, U_{\max}]$ (in our case $[U_\infty, U_s]$ or $[U_s, U_\infty]$), often called the 'physical' sheet. It is easy to show that there are no singularities of the function $\tilde{G}(c)$

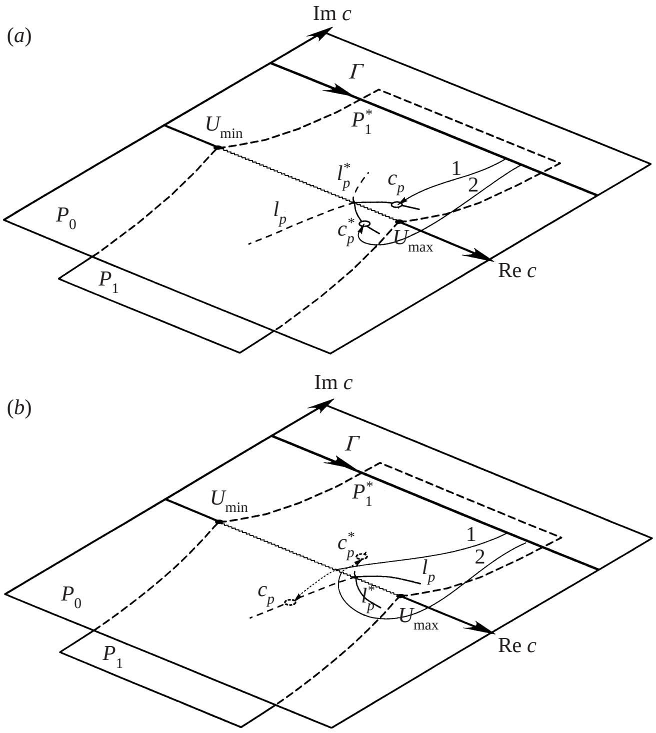

FIGURE 2. Sheets of the analytical continuation: (*a*) c-plane for the case when the profile has an inflection point and both an unstable mode and the conjugate one exist. The corresponding poles c_p and c_p^* are located on the 'physical' sheet P_0. A continuous deformation of the velocity profile moves the poles along the lines l_p and l_p^*, respectively. (*b*) If because of the continuous deformation of the profile the inflection point disappears, the poles cross the cut $[U_{\min}, U_{\max}]$ (without merging) and do not disappear, but pass onto the other sheets P_1 and P_1^*. Lines indicated by arrows show the analytical continuation from the initial contour Γ to the vicinity of the poles in both cases.

on P_0, except, maybe, a few poles (figure 2*a*). These poles, if they exist, are located within the so-called Howard's semicircle (e.g. Drazin & Reid 1981).

If a pole c_p exists on the upper half-plane of P_0, then the corresponding complex conjugate pole c_p^* necessarily exists and is obviously situated on the lower half-plane of the physical sheet P_0 (see figure 2*a*). The residue at the conjugate pole c_p^* corresponds to a decaying eigen mode. The latter is commonly neglected. (Obviously the decaying mode contribution is exponentially small. Moreover, such modes are known to be structurally unstable with respect to introducing an infinitesimal viscosity. That is, in contrast to the growing modes, they do not represent the limit of the corresponding modes of the Orr–Sommerfeld equation when the Reynolds number tends to infinity (e.g. Lin 1955).)

If we deform the initial contour Γ downward (recall that the integrand of the inverse Laplace transform (2.11) decays downward for $t > 0$ owing to the factor $\exp(-\mathrm{i}kct)$). Then it splits into a set of contours around all the poles on the physical sheet P_0 and a contour around the cut $[U_{\min}, U_{\max}]$. The contribution due to each pole can be found by calculating their residues. Thus, the solution describing evolution of an initial delta pulse is represented as a sum of growing and decaying modes and an integral around the cut. The latter describes the contribution of the continuous spectrum modes which is known to decay as t^{-2} for large time for any smooth initial perturbation.

If we deform a profile with an inflection point (or vary appropriately the wavenumber) the poles c_p and c_p^* move on the P_0 sheet and, if the inflection point disappears (or the wavenumber becomes large enough), they reach and cross the cut (see figure 2*b*). (It is possible to show that under the variation of the wavenumber the poles must cross the cut precisely at the inflection point. Notice also, that the pole and the conjugate pole do not merge as they are at the opposite branches of the cut.) After crossing the cut, the poles move onto sheets P_1 and P_1^* which are the analytical continuations through the cut from above and from below, respectively.

In the flows without inflection points there are no poles on the physical sheet P_0 (see figure 2*b*), therefore only the integral around the cut contributes to $G(c)$, that is, in full accordance with the common wisdom, the continuous spectrum determines the evolution of any initial perturbation. Hence, we might expect the same t^{-2} decay. As we show below, although such decay indeed manifests itself at the final stage of evolution, there is a wide time interval specified in the next section where the evolution is quite different and is determined by the residue of the Landau pole c_p. Technically speaking, we show in the next section with what accuracy the integral over the cut is approximated well by the residue in the pole c_p. The conjugated pole c_p^* on P_1^* does not contribute since the integration contour is moved and continued from above and, thus, 'catches' the singularities of sheet P_1 only, but not those of P_1^*. The fact that the integration contour is moved and continued from above follows directly from the causality principle, explicitly or implicitly necessarily employed in consideration of initial problems.

3.4. *Other singularities of the Green's function*

Based on the analysis of the singularities of integral (3.2) that we carried out in § 3.2, we can expect the logarithmic singularities in the points corresponding to the integration limits of the integrals I_z, I_h and I_B, i.e. at the points $c = U_z$, $c = U_h$ and $c = U_s$. We might expect a singularity at $c = U_B$ as well, but, since B is a fictitious parameter, this singularity is absent in the exact formula. If we retain a finite number of terms of the series in ϵ, say n, it is possible to check that this singularity appears only in the order $O(\epsilon^{n+1})$ and, therefore, we do not need to consider it here.

If we take into account higher-order approximations of the Green's function we also obtain a singularity at the point U_∞ (see function χ in (A 13*d*)), nevertheless, it is possible to show that the contribution of this point is of higher order.

The types of singularities at the points U_s, U_z and U_z subject to further analysis are different as they can be either only in the numerator (U_z,U_h) or both in the numerator and denominator, as is the case for U_s. It is easy to see that the combination $V_z I_z$ does not result in a pole at the point U_z but yields only a logarithmic singularity.

All of the singularities and the coefficients with which they enter into the Green's function $\tilde{G}$ are summarized in table 1.

4. Large-time asymptotics of long-wave perturbations

In this section we analyse the evolution of arbitrary initial long-wave perturbations capitalizing on the derived explicit formulae for the singularities of the Green's function (3.1) summarized in table 1.

To study large-time asymptotics of the solutions of the initial-value problem (2.4) we make cuts from each branch point vertically downwards as this is the direction

Point	Type of singularity	Coefficient in $\tilde{G}$
c_p	$\dfrac{1}{c-c_p}$	$\mathrm{i}V_\infty^2 V_z I_z V_s I_h\big\vert_{c=c_p}$
U_z	$V_z \log V_z$	$\dfrac{U_z''}{\mathrm{i}k(U_z')^3}\left[\theta(h-z)+\dfrac{kV_\infty^2}{c-c_p}V_s I_h\right]\Big\vert_{c=U_z}$
U_h	$\dfrac{1}{V_h}+\dfrac{U_h''}{(U_h')^2}\log V_h$	$\dfrac{V_z}{\mathrm{i}kU_h'}\left[\theta(z-h)+\dfrac{kV_\infty^2}{(c-c_p)U_h'}V_s V_z I_z\right]\Big\vert_{c=U_h}$
U_s	$V_s^2 \log V_s$	$\dfrac{\mathrm{i}V_z U_s''}{k^3 U_s' V_\infty^4}\Big\vert_{c=U_s}$

TABLE 1. Types of singularities and their coefficients ($\theta(x)$ is the Heaviside unit step function).

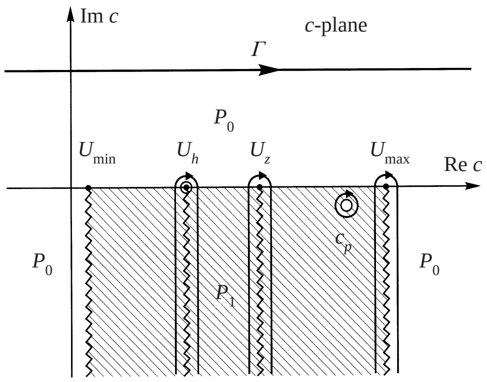

FIGURE 3. Deformation of the integration contour. Bold lines depict the initial integration contour Γ and the deformed contour representing a set of four integration contours Γ_s, Γ_p, Γ_z and Γ_h encompassing the Green's function $\tilde{G}(c)$ singular points U_s, c_p, U_z and U_h; saw-tooth lines denote cuts from the singular points. The singular point at infinity U_∞ is excluded since it does not contribute in the leading-order approximation.

of the steepest descent of the integrand in (2.11) due to the factor $\exp(-\mathrm{i}kct)$. Thus, we consider a sheet consisting of parts of the P_0 and P_1 sheets. All the singularities such as V_z, V_h which are hidden, if the analytical continuation onto the P_0 sheet is considered, become apparent.

Then, we move the initial contour Γ downwards, deform it, and split it into the four contours $\Gamma_p, \Gamma_z, \Gamma_h$ and Γ_s encompassing each singularity and passing along the vertical cuts for branch points (figure 3).

We consider consecutively contributions of each singular point and the characteristic time when its asymptotic representation is valid for the Green's function. Then, we calculate its convolution with an arbitrary long-wave initial distribution of the vorticity ω_0 satisfying (2.6). The derivation for the points U_s, U_z and U_h is described in Appendix B in detail. In this section, we present final simplified formulae for the contribution of the singularities in the velocity components u and w and vorticity ω. We denote by subscript p, z, h and s contributions due to the points c_p, U_z, U_h and U_s, respectively. (We recall that the singularity at infinity U_∞ is not considered since its contribution is of higher order in k.)

4.1. *Residue in the pole. Quasi-modes*

We calculate the residue straightforwardly and obtain the following leading term of the expansion of G_p in k

$$G_p = \mathrm{i}k^2 \frac{\Delta U^4}{U_s'} \, [V_z(c_p) I_z(c_p)] \, I_h(c_p) \exp(-\mathrm{i}kc_p t), \tag{4.1}$$

taking into account the fact that $V_s(c_p) = k\Delta U^2 (U_s')^{-1}$. Expression (4.1) describes a wave with the complex phase velocity c_p and vertical velocity profile $V_z(c_p)I_z(c_p)$.

Consider the integral $I_z(c_p)$ as a function of z. By virtue of (3.3), the behaviour of $I_z(c_p)$ for small $z \sim z_r$ is mainly determined by the singular terms. For intermediate $z \sim H$ the non-singular term J_z in (3.3*b*) should be taken into account. In this range, we can simplify this term by approximating function V_z in the denominator of the integrand for J_z by the constant $V_z(c_p) \approx V_\infty(U_s) \equiv U_\infty - U_s$. As a result, we obtain an explicit approximate formula

$$I_z(c_p) \simeq \frac{1}{V_s U_s'} - \frac{1}{V_z U_z'} + \frac{U_r''}{(U_s')^3} \log \frac{V_s}{V_z} - \frac{U_r''}{(U_s')^3} \frac{U_z - U_s}{U_\infty - U_s} + \frac{U_s^{-1} - U_z^{-1}}{U_\infty - U_s}. \tag{4.2}$$

The smaller k, the better is this approximation. Since c_p is close to U_s we can substitute U_s' instead of U_r'. The function $I_z(c_p)$ attains its maximum

$$\max_z \{I_z(c_p)\} = \frac{1}{\mathrm{i}c_i U_s'} \simeq \frac{\mathrm{i}(U_s')^3}{k^2 \pi \Delta U^4 U_r''}$$

at $z = z_r$, then sharply decreases down to a value of the order of $(-c_r U_s')^{-1} \approx k^{-1}\Delta U^{-2}$ determined by the first term of (4.2). Using this approximation, we can estimate the integral in the convolution of the Green's function and the initial distribution of vorticity $\omega_0(z)$

$$\int_0^\infty I_h(c_p)\omega_0(h)\,\mathrm{d}h \simeq \frac{1}{k\Delta U^2} \int_0^\infty \omega_0(h)\,\mathrm{d}h = \frac{1}{k\Delta U^2}(-u_0(0) + O(k^2)),$$

where $u_0 = -\partial_z \psi_0$ is the horizontal velocity component of the initial disturbance. The integration over small $h \sim z_r$ does not contribute except in the special case $\int_0^\infty \omega_0(h) = 0$.

Eventually, we can present the formulae for the pole contribution into asymptotics of the initial problem in terms of the field components

$$w_p = \mathrm{i}k\psi_p = \frac{-\mathrm{i}k^2 \Delta U^2}{U_s'} [V_z(c_p) I_z(c_p)] \exp(-\mathrm{i}kc_p t) \int_0^\infty \omega_0(h)\,\mathrm{d}h, \tag{4.3a}$$

$$u_p = \frac{k\Delta U^2}{U_s'} [U_z' I_z(c_p) + V_z^{-1}(c_p)] \exp(-\mathrm{i}kc_p t) \int_0^\infty \omega_0(h)\,\mathrm{d}h, \tag{4.3b}$$

$$\omega_p = \frac{-k\Delta U^2}{U_s'} [U_z'' I_z(c_p)] \exp(-\mathrm{i}kc_p t) \int_0^\infty \omega_0(h)\,\mathrm{d}h. \tag{4.3c}$$

Note, that if $c_i < 0$, we must take different branches of the logarithmic function in $I_z(c_p)$ (the third term in (4.2)), depending on whether z is greater or smaller than the critical layer height z_r. (We recall that we distinguish the real critical layer z_r: $U(z_r) = \mathrm{Re}\, c_p$, and the complex critical layer z_c: $U(z_c) = c_p$.) Therefore, the residue of G_p has a small jump at this point (see figure 8 in Briggs *et al.* 1970) that results in the jumps in the velocity and vorticity components:

$$\Delta w_p = \frac{2\mathrm{i}\pi^2 k^4 (U_r'')^2 \Delta U^6}{(U_s')^8} \exp(-\mathrm{i}ktc_p) \int_0^\infty \omega_0(h)\,\mathrm{d}h \sim \epsilon^3\, w_p(z \sim H), \tag{4.4a}$$

$$\Delta u_p = \frac{2\mathrm{i}\pi k \Delta U^2 U_r''}{(U_s')^3} \exp(-\mathrm{i}ktc_p) \int_0^\infty \omega_0(h)\,\mathrm{d}h \sim \epsilon\, u_p(z \lesssim H), \tag{4.4b}$$

$$\Delta \omega_p = -\frac{2\mathrm{i}\pi k \Delta U^2 (U_r'')^2}{(U_s')^4} \exp(-\mathrm{i}ktc_p) \int_0^\infty \omega_0(h)\,\mathrm{d}h \sim \epsilon\, \omega_p(z \lesssim H). \tag{4.4c}$$

Owing to these jumps it is impossible to obtain a continuous smooth solution due to the pole alone satisfying both the boundary conditions and the Rayleigh equation in all the points. Thus, if $c_i < 0$, the residue in the pole c_p does not correspond to a true eigen mode and that is why this solution does not contradict the Rayleigh theorem (see also Briggs *et al.* 1970 for more detail). However, since the residue in the pole c_p does contribute significantly to the asymptotics and, moreover, as we show below, its contribution dominates over significant time intervals and behaves as a mode, it makes sense to treat it like a mode and call it a mode as well. To reflect the mathematical peculiarity of such objects we use the term quasi-modes coined by Briggs *et al.* (1970). However, to be of practical use, the mode's jumps should be small. We show below that in our context these jumps are indeed small (compared to the typical values of w_p, u_p and ω_p in the layer $z \lesssim H$, see (4.7) below).

We stress, that the total velocity and vorticity fields remain continuous and smooth as expected for a solution of an initial problem with a smooth initial distribution: the jumps of w_p, u_p and ω_p in the point z_r are equal in modulo but opposite in sign to the jumps of w_z, u_z and ω_z (see §4.2) owing to the critical layer singularity $c = U(z_c)$.

Note, also, that we cannot obtain other field components, say, u_p and ω_p, by straightforwardly differentiating w_p, it is necessary to calculate the residues in c_p of $\tilde{u}(c,z)$, $\tilde{\omega}(c,z)$. The same is true for the u_z and ω_z. The components $\tilde{u}$ and $\tilde{\omega}$ have to be expressed through derivatives of the Green's function:

$$\tilde{u} = \int_0^\infty (-\partial_z \tilde{G}(z|h))\,\omega_0(h)\,\mathrm{d}h, \quad \tilde{\omega} = \int_0^\infty (\partial_z^2 - k^2)\tilde{G}(z|h)\,\omega_0(h)\,\mathrm{d}h. \tag{4.5}$$

It is easy show that the derivatives $\partial_z \tilde{G}$ and $\partial_z^2 \tilde{G}$ have singularities in the same points as $\tilde{G}$ and these singularities can be studied in the same manner.

The ultimate simplifications

Notice, that since the maximal contribution into integral $I_z(c_p)$ is provided by integration in the neighbourhood of $z \sim z_r$, we can further simplify this integral approximating $U_z \approx U_s + U_s' z$. Then we have

$$I_z(c_p) \approx \frac{z}{(U_s + U_s' z - c_p)(U_s - c_p)}. \tag{4.6}$$

Comparison with the exact function shows that (4.6) satisfactorily quantitatively describes the integral in the considered approximation (but not qualitatively as the small jump is removed).

Outside the immediate vicinity of the surface, i.e. for $z \gg z_r$, we can further simplify the expressions for the field components. The ultimate formulae describe weakly decaying monochromatic waves characterized by very simple smooth field dependence on z with the amplitude proportional to the first moment of the initial distribution of vorticity

$$w_p = \mathrm{i}k\frac{U_s - U_z}{U_s'}[\exp(-\mathrm{i}kc_pt)]\exp(-kz)\int_0^\infty \omega_0(h)\,\mathrm{d}h, \tag{4.7a}$$

$$u_p = \frac{U_z'}{U_s'}[\exp(-\mathrm{i}kc_pt)]\int_0^\infty \omega_0(h)\,\mathrm{d}h, \tag{4.7b}$$

$$\omega_p = -\frac{U_z''}{U_s'}[\exp(-\mathrm{i}kc_pt)]\int_0^\infty \omega_0(h)\,\mathrm{d}h. \tag{4.7c}$$

The small spikes and jumps are all in the neglected higher orders. From (4.7) we can see that the vertical velocity increases as with z and attains its maximum at $z \sim H$ and then decreases owing to the factor $\exp(-kz)$ (see comments on this factor at the end of Appendix A). The horizontal velocity attains its maximum at the surface and remains of the same order while $z \lesssim H$. Position of the maximum for the vorticity ω_p depends on the velocity profile and is determined by maximum of U''.

4.2. *Contribution of the singularity U_z*

Non-modal contributions of the singularity $c = U_z$ to the velocity and vorticity components can be described by the following asymptotic formulae (see Appendix B.2):

$$w_z = \frac{\mathrm{i}U_z''}{kt^2(U_z')^3}\exp(-\mathrm{i}kU_zt)\int_z^\infty \omega_0(h)\,\mathrm{d}h + w_z^a, \tag{4.8a}$$

$$u_z = \frac{\mathrm{i}U_z''}{kt(U_z')^2}\exp(-\mathrm{i}kU_zt)\int_z^\infty \omega_0(h)\,\mathrm{d}h + u_z^a, \tag{4.8b}$$

$$\omega_z = -\frac{U_z''}{U_z'}\exp(-\mathrm{i}kU_zt)\int_z^\infty \omega_0(h)\,\mathrm{d}h + \omega_z^a. \tag{4.8c}$$

owing to the small factor k, the last terms are essential near the critical layer $z \sim z_r$ only:

$$w_z^a = \frac{kU_r''\Delta U^2}{(U_s')^4}\left[\frac{\exp(-\mathrm{i}ktU_z)}{t} - \mathrm{i}k(U_z - c_p)\,E_1\exp(-\mathrm{i}ktc_p)\right]\int_0^\infty \omega_0(h)\,\mathrm{d}h, \tag{4.9a}$$

$$u_z^a = \frac{kU_r''\Delta U^2}{(U_s')^3}E_1\exp(-\mathrm{i}ktc_p)\int_0^\infty \omega_0(h)\,\mathrm{d}h, \tag{4.9b}$$

$$\omega_z^a = \frac{kU_r''\Delta U^2}{(U_s')^4}\left[U_z''E_1\exp(-\mathrm{i}ktc_p) - \frac{(U_s')^2}{(U_z - c_p)}\exp(-\mathrm{i}ktU_z)\right]\int_0^\infty \omega_0(h)\,\mathrm{d}h, \tag{4.9c}$$

where

$$E_1(Z) = \int_Z^\infty \mathrm{e}^{-z}\,\mathrm{d}z$$

is the exponential integral function. Throughout this work it has the same argument $E_1 = E_1[\mathrm{i}kt(U_z - c_p)]$. Different branches of this function are taken for the cases $z < z_r$ and $z > z_r$ if $c_i < 0$, therefore, the functions w_z, u_z and ω_z have jumps and, as is mentioned above, those jumps exactly compensate the jumps (4.4) in w_p, u_p and ω_p, respectively, ensuring smoothness of the total field.

The derived formulae (4.8)–(4.9) become valid for sufficiently large time:

$$t \gg t_z \sim \frac{1}{|U_s'|}. \tag{4.10}$$

4.3. *Contribution of the singularity U_h*

Contribution of the singularity U_h to the Green's function is derived in Appendix B.3. Its convolution with the initial condition is given by the following asymptotic formulae

$$w_h \simeq w_{h,z} + w_{h,s} = \frac{-\mathrm{i}}{kt^2}\frac{\omega_0(z)}{(U_z')^2}\exp(-\mathrm{i}kU_z t) + \frac{(U_s-U_z)U_s'\omega_0(0)}{\mathrm{i}k^2t^2\Delta U^2}\exp(-\mathrm{i}kU_s t), \tag{4.11a}$$

$$u_h \simeq u_{h,z} + u_{h,s} = \frac{-\mathrm{i}}{kt}\frac{\omega_0(z)}{U_z'}\exp(-\mathrm{i}kU_z t) - \frac{U_z'U_s'\omega_0(0)}{k^3t^2\Delta U^2}\exp(-\mathrm{i}kU_s t), \tag{4.11b}$$

$$\omega_h \simeq \omega_{h,z} + \omega_{h,s} = \omega_0(z)\exp(-\mathrm{i}kU_z t) - \frac{U_z''U_s'\omega_0(0)}{\mathrm{i}k^4t^2\Delta U^2}\exp(-\mathrm{i}kU_s t). \tag{4.11c}$$

First terms in (4.11) are valid when

$$t \gg t_{h,z} \sim \max_z \frac{|U_z''|}{k(U_z')^2}. \tag{4.12a}$$

The second terms in (4.11) are valid for essentially greater time

$$t \gg t_{h,s} \sim \frac{|U_s'|}{k^2\Delta U^2}, \tag{4.12b}$$

but they should be taken into account for vertical velocity only provided $\omega_0(0) \neq 0$. Numerical computation shows that the second terms in (4.11) do not dominate even for smaller time.

4.4. *Contribution of the singularity U_s*

The contribution of U_s is given by the following asymptotic formulae (see Appendix B.1):

$$w_s = \frac{-2U_s''(U_s-U_z)}{k^4t^3U_s'\Delta U^4}\exp(-\mathrm{i}kU_s t)\int_0^\infty \omega_0(h)\,\mathrm{d}h, \tag{4.13}$$

$$u_s = \frac{2\mathrm{i}U_s''U_z'}{k^5t^3U_s'\Delta U^4}\exp(-\mathrm{i}kU_s t)\int_0^\infty \omega_0(h)\,\mathrm{d}h, \tag{4.14}$$

$$\omega_s = \frac{-2\mathrm{i}U_s''U_z''}{k^5t^3U_s'\Delta U^4}\exp(-\mathrm{i}kU_s t)\int_0^\infty \omega_0(h)\,\mathrm{d}h, \tag{4.15}$$

which are valid when

$$t \gg t_s \sim \frac{U_s''}{(U_s')^2k}. \tag{4.16}$$

4.5. *Quasi-modes as intermediate asymptotics of smooth initial perturbations*

Now we compare the contribution of all the singularities of the Green's function into all field components. We can split the total perturbation field into two parts: the first one due the residue at the pole (we refer to it as the quasi-mode (QM), so $w_p \equiv w_{\mathrm{QM}}$, etc.) and the remainder (we call it the 'tail' for simplicity)

$$\begin{array}{lllllllll}
w = & w_{\mathrm{QM}} & + \; w_{\mathrm{tail}}, & w_{\mathrm{tail}} = & w_z & + \; w_{h,z} & + \; w_{h,s} & + \; w_s, \\
 & \sim \exp(-kc_i t) & \;\sim t^{-2} & & \sim t^{-2} & \sim t^{-2} & \sim t^{-2} & \sim t^{-3} \\
u = & u_{\mathrm{QM}} & + \; u_{\mathrm{tail}}, & u_{\mathrm{tail}} = & u_z & + \; u_{h,z} & + \; u_{h,s} & + \; u_s, \\
 & \sim \exp(-kc_i t) & \;\sim t^{-1} & & \sim t^{-1} & \sim t^{-1} & \sim t^{-2} & \sim t^{-3} \\
\omega = & \omega_{\mathrm{QM}} & + \; \omega_{\mathrm{tail}}, & \omega_{\mathrm{tail}} = & \omega_z & + \; \omega_{h,z} & + \; \omega_{h,s} & + \; \omega_s, \\
 & \sim \exp(-kc_i t) & \;\sim t^{-0} & & \sim t^{-0} & \sim t^{-0} & \sim t^{-2} & \sim t^{-3}
\end{array}$$

where specific time asymptotics of each contribution are explicitly shown. Thus, the QM-part of the disturbance decays exponentially, whereas velocity components of the tail decay algebraically. Therefore, the QM-part can dominate in the velocity field over a certain interval of time. On the contrary, the vorticity distribution is never dominated by the quasi-mode unless a special class of initial disturbances is considered.

Before attempting to find the time interval of the quasi-mode dominance we should establish a criterion. Obviously, the answer would vary for different components and for different z. For example, as we mentioned, it never dominates in the vorticity distribution, because vorticity emphasizes the field components of small vertical scales while the quasi-mode has the vertical scale of the boundary layer. However, if we are interested in the evolution of the field in a certain integral sense, say, only in the components of $O(1)$ vertical scale, then the small-scale field components being filtered out, the quasi-mode becomes more emphasized. Even in terms of vorticity (understood in such a coarse-grained sense) we find, tracing behaviour of the integrals of the type,

$$\int_0^{\infty} f(z)\omega(z)\,\mathrm{d}z,$$

where $f(z)$ is a smooth function, that the QM contribution prevails in a certain time interval. In terms of the horizontal velocity, the QM-part cannot prevail in the vicinity of the critical layer (where the non-modal term u_a is essential).

The most obvious and sufficiently universal integral criterion enabling us to compare different parts of the solution is the disturbance energy, defined as

$$E = \frac{1}{2}\int_0^{+\infty} \langle |\mathrm{Re}\, u|^2 + |\mathrm{Re}\, w|^2\rangle\,\mathrm{d}z, \tag{4.17}$$

where $\langle\ldots\rangle$ denotes averaging over x. It is easy to see that the second term of the integrand is $|\mathrm{Re}\, w|^2 \sim \epsilon^2|\mathrm{Re}\, u|^2)$ for long waves and is, therefore, negligible. Using our previous results, we present the time asymptotics for both parts of the horizontal velocity retaining only the leading terms in a more explicit way:

$$u_{\mathrm{QM}} \equiv u_p \approx \frac{U_z'}{U_s'}[\exp(\mathrm{i}kx - \mathrm{i}kc_p t)]\int_0^{\infty} \omega_0(h)\,\mathrm{d}h,$$

$$u_{\mathrm{tail}} = u_z + u_{h,z} \approx \frac{-\mathrm{i}}{kt}\left(\frac{\int_z^{\infty}\omega_0(h)\,\mathrm{d}h}{U_z'}\right)' \exp(\mathrm{i}kx - \mathrm{i}kU_z t),$$

For the energies of the two parts we immediately find

$$\begin{aligned} E_{\mathrm{QM}} &= \frac{1}{2}\int_0^{+\infty}\langle |\mathrm{Re}\, u_{\mathrm{QM}}|^2\rangle\,\mathrm{d}z \\ &= \frac{1}{4}\int_0^{\infty}\left(\frac{U'}{U_s'}\right)^2 \mathrm{d}z \left(\int_0^{\infty}|\omega_0(z)|\,\mathrm{d}z\right)^2 \exp(-2c_i kt) \propto \exp(-2kc_i t), \end{aligned}$$

$$E_{\mathrm{tail}} = \frac{1}{2}\int_0^{+\infty}\langle |\mathrm{Re}\, u_{\mathrm{tail}}|^2\rangle\,\mathrm{d}z = \frac{1}{4k^2t^2}\int_0^{\infty}\left[\left(\frac{\int_z^{\infty}\omega_0(h)\,\mathrm{d}h}{U_z'}\right)'\right]^2 \mathrm{d}z \propto \frac{1}{t^2}.$$

Thus, in terms of energy the QM and 'tail' parts have the same asymptotic decay as in terms of stream function or vertical velocity.

Although the energy E is a non-additive value, nevertheless it is approximately equal to the sum of E_{QM} and E_{tail}. It is easy to show that

$$E-(E_{\mathrm{QM}}+E_{\mathrm{tail}})=\frac{1}{2}\int_0^{+\infty}\langle|\mathrm{Re}(u_{\mathrm{QM}}\,u_{\mathrm{tail}})|\rangle\,\mathrm{d}z \ll E_{\mathrm{QM}},E_{\mathrm{tail}}$$

for sufficiently large times. This is due to the oscillatory behaviour in z of $u_{\mathrm{tail}} \propto \exp(-\mathrm{i}kU_z t)$, whereas the u_{QM} characteristic lengthscale is of the order H. Thus,

$$E \approx E_{\mathrm{QM}}+E_{\mathrm{tail}}.$$

It is convenient to use non-dimensional variables

$$\bar{t}=t|U_s'|, \tag{4.18a}$$
$$\bar{k}=kH\equiv\epsilon, \tag{4.18b}$$
$$\bar{z}=z/H, \tag{4.18c}$$

and to specify the amplitude of the initial disturbance setting

$$\int_0^{\infty}|\omega_0(z)|\,\mathrm{d}z\sim 1.$$

Then, in the generic case ($U_s''\neq 0$), we obtain

$$E_{\mathrm{QM}}\sim\exp(-2\kappa\bar{k}^3\bar{t}\,),$$
$$E_{\mathrm{tail}}\sim\bar{k}^{-2}\bar{t}^{-2},$$

where $\kappa=\pi|U_s''\Delta U(U_s')^{-2}|$ is a non-dimensional parameter of the order of unity. In the important degenerate case of the Blasius profile we have

$$E_{\mathrm{QM}}\sim\exp(-2\kappa_{BL}\bar{k}^4\bar{t}),$$

where $\kappa_{\mathrm{BL}}=\pi|U_s'''\Delta U_\infty^2(U_s')^{-3}|\approx 8$.

Comparing two functions $\exp(-2\kappa\bar{k}^3\bar{t})$ and $\bar{k}^{-2}\bar{t}^{-2}$, it is easy see that for sufficiently small $\bar{k}$ they intersect twice, say, at $\bar{t}_1$ and $\bar{t}_2$. The interval where the QM contribution dominates, i.e. $E_{\mathrm{QM}}\gg E_{\mathrm{tail}}$, is bounded by these points: $\bar{t}_1\ll\bar{t}\ll\bar{t}_2$. The intersection points can be expressed via the Lambert functions (solutions of the equation $x\exp(x)=y$), however, in the limit of small $\bar{k}$ that we are interested in, it is sufficient to use simple estimates:

$$\bar{t}_1\sim\bar{k}^{-1},\ \bar{t}_2\sim\bar{k}^{-3}\log(1/\bar{k}). \tag{4.19}$$

Now we can also quantify how strongly the E_{QM} part dominates:

$$R=\frac{E_{\mathrm{QM}}}{E_{\mathrm{tail}}},\quad R_{\mathrm{max}}\sim R_{\mathrm{mean}}=\frac{1}{\bar{t}_2-\bar{t}_1}\int_{\bar{t}_1}^{\bar{t}_2}R\,\mathrm{d}t\sim\bar{k}^{-4}. \tag{4.20}$$

Thus, we have shown that in the generic case for small $\bar{k}$ there is indeed a wide interval where the contribution due to the pole strongly dominates in the integral (energy) sense.

Note that, for the degenerate cases ($U_s''=0$), with the Blasius profile being the most notable example, both the interval of the quasi-mode dominance is obviously wider

$$\bar{t}_1\sim\bar{k}^{-1},\ \bar{t}_2\sim\bar{k}^{-4}\log(1/\bar{k}), \tag{4.21}$$

and the quasi-mode is even more pronounced

$$R = \frac{E_{\mathrm{QM}}}{E_{\mathrm{tail}}}, \quad R_{\mathrm{mean}} = \frac{1}{\bar{t}_2 - \bar{t}_1} \int_{\bar{t}_1}^{\bar{t}_2} R \, \mathrm{d}t \sim \bar{k}^{-6}. \tag{4.22}$$

The asymptotic analysis of evolution of an initial perturbation that we carried out, provides a clear picture of it, especially transparent in terms of $E(t)$. First, there is an 'initial transition' period $\bar{t} \lesssim \bar{k}^{-1}$, when the asymptotic formulae derived are not yet valid, while the initial disturbance energy $E(t)$ remains of the order of unity. Then, in the intermediate asymptotics interval $\bar{k}^{-1} \ll \bar{t} \ll \bar{k}^{-3} \log(1/\bar{k})$, $E(t)$ is very close to E_{QM} and is, therefore, decaying as $\exp(-2\kappa\bar{k}^3\bar{t})$. At the end of the interval, the energy is $O(\bar{k}^{-4})$ of the initial energy. At even greater times, $E(t)$ is no longer close to E_{QM} and owing to the tail contribution becoming more and more noticeable, its decay gradually tends to a final stage of the expected t^{-2} decay (see plots in figure 7).

We note that behaviour of almost any other integral characteristics of the perturbation, except enstrophy, is qualitatively the same.

5. Beyond the long-wave asymptotics

Our asymptotic analysis was based on the long-wave approximation and, thus, employed heavily the smallness of $\bar{k}$. We have established the existence of the specific pole lying close to the real axis on a particular sheet of complex plane c for an arbitrary boundary-layer-type shear flow. We also showed that the contribution due to this pole to the solution of arbitrary initial problem, the quasi-mode, prevails in the wide time interval found asymptotically.

In this section, we address the fundamental question: What happens beyond the range of applicability of the derived asymptotic formulae?

In § 5.1, we employ numerics to find the exact positions of the pole on complex plane c for a number of profiles of interest for applications. We check our asymptotic theory and obtain a new insight into the role of this singularity. In § 5.2, we investigate the evolutionary problem numerically and find that the asymptotic theory works fairly well.

5.1. *Quasi-modes in various flows*

The position of the pole on complex plane c specifies both the dispersion relation of the quasi-mode, i.e. $\mathrm{Re}\, c(k)$, and its characteristic time of existence through $\mathrm{Im}\, c(k)$. In this subsection, we compute the exact dependence $c(k)$ for a number of profiles of interest for applications.

In this section, we consider flows normalized for convenience in a uniform way as follows

$$U_s = 1, \tag{5.1a}$$

$$U_s' = -1, \tag{5.1b}$$

$$U_\infty = 0. \tag{5.1c}$$

We can always choose the appropriate reference-frame and length units for any boundary-layer-type flow (if ΔU is finite). Actually, we use lengthscale H for coordinate and U_s for the velocity. Thus $H = 1$ and $k = \bar{k} = \epsilon$.

Exponential (EX). The exponential profile $U = \exp(-z)$ appears in a number of real-world problems, say, for boundary layers with suction, but is mostly used as a model profile having the extreme simplicity as its decisive advantage and justification.

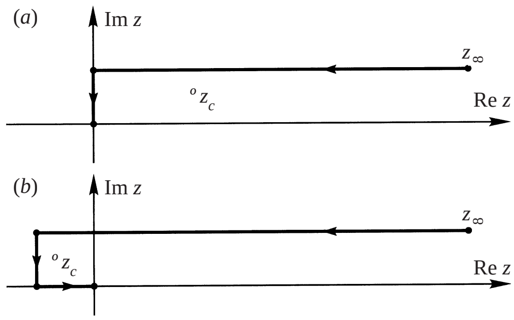

FIGURE 4. Integration path for solving the modified Riccati type equation: (*a*) $\mathrm{Re}\, z_c > 0.1$; (*b*) $\mathrm{Re}\, z_c < 0.1$.

Falkner–Skan (FS). The laminar wind-driven surface current profile induced by the stationary wind stress is described by one of the family of the so-called Falkner–Skan profiles (Dupont & Caulliez 1993). In the normalized form $U(z) = F_{\mathrm{FS}}(z)$, where $F_{\mathrm{FS}}(z) = f'(z\lambda_{\mathrm{FS}})/\lambda_{\mathrm{FS}}$ where $\lambda_{\mathrm{FS}} \approx 1.298$ is introduced to satisfy convention (5.1), while $f(z)$ is the solution of the boundary-value problem

$$\begin{aligned} &3f''' + 2ff'' - (f')^2 = 0, \\ &f(0) = 0, \quad f''(0) = -1, \quad f'(\zeta \to +\infty) \to 0. \end{aligned} \tag{5.2}$$

Blasius (BS). The Blasius profile given in most textbooks on hydrodynamics in its normalized form $U(z) = F_{\mathrm{BS}}(z) = f'(z\lambda_{\mathrm{BS}})/\lambda_{\mathrm{BS}}$ where $\lambda_{\mathrm{BS}} \approx 1.821$ is expressed via the solution $f(z)$ of similar boundary-value problems

$$\begin{aligned} &-f''' + 3ff'' - (f')^2 = 0, \\ &f(0) = 0, \quad f'(0) = -1, \quad f'(\zeta \to +\infty) \to 0. \end{aligned} \tag{5.3}$$

Logarithmic (LG). The logarithmic profile $U = 1 - \log(1 + z)$ describes turbulent flows near a rough infinite wall (e.g. Tennekes & Lumley 1972). It diverges at infinity and therefore does not fit into the class of profiles that we applied our asymptotic analysis to and does not satisfy (5.1*c*). We, nevertheless, consider it here only to show that the quasi-mode concept remains relevant for such a class of flows as well.

For each converging flow in the list we also provide the explicit expressions for the long-wave asymptotics for the pole summarized below.

EX: The exponential profile: $U = \exp(z)$, $c_p = 1 - k - \mathrm{i}\kappa_{\mathrm{EX}} k^2$, $\kappa_{\mathrm{EX}} = \pi$.

FS: The Falkner–Skan profile: $c_p = 1 - k - \mathrm{i}\kappa_{\mathrm{FS}} k^2$, $\kappa_{\mathrm{FS}} = \pi 0.726\ldots = 2.28\ldots$.

BS: The Blasius profile: $c_p = 1 - k - \mathrm{i}\kappa_{\mathrm{BS}} k^3$, $\kappa_{\mathrm{BS}} = \pi 2.54\ldots = 7.99$.

To compute the position of the pole, we transform the Rayleigh equation into the modified Riccati type equation by the substitution $\tan(\alpha(z)) = \psi'/\psi$:

$$\alpha' + 1 = \cos^2\alpha[1 + k^2 + (U - c)^{-1} U'']. \tag{5.4a}$$

The equation is integrated numerically as an initial problem with the initial condition:

$$\tan(\alpha(z_\infty)) = -k, \tag{5.4b}$$

along the path lying on the complex z-plane shown in figure 4.

The path includes two (if $\mathrm{Re}\, z_c > 0.1$) or three segments encompassing the pole at a distance not closer than 0.1 (this particular value is chosen for optimizing the numerical routine). The initial point z_∞ instead of infinity is taken to be $(k^{-2} + 5^2)^{1/2}$ (this value is found by trial and error to ensure the desired accuracy of 10^{-8}). The

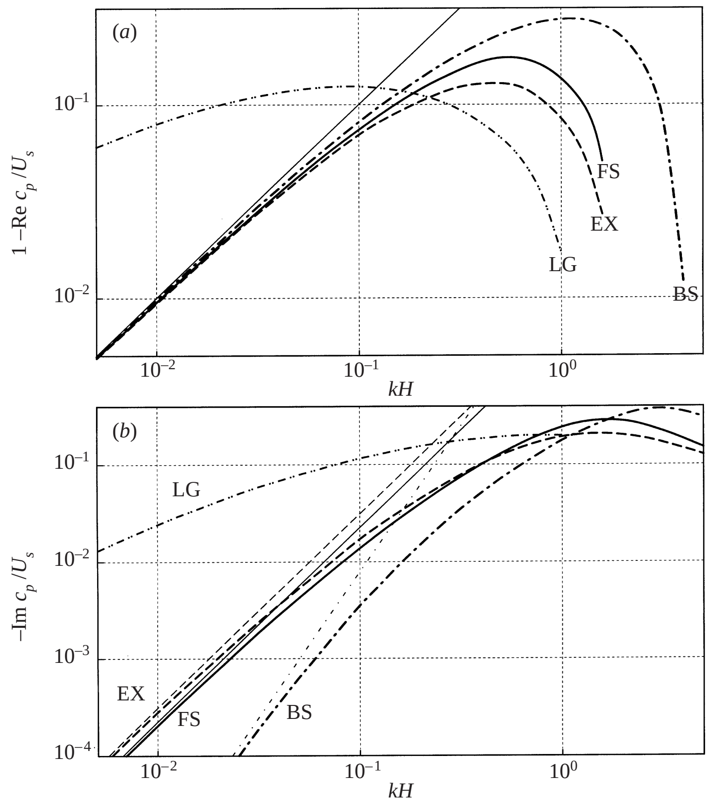

FIGURE 5. Dispersion curves for quasi-mode for various flows ((*a*) real part; (*b*) imaginary part): EX, exponential; FS, Falkner–Scan; BS, Blasius profile; LG, logarithmic profile; bold and thin lines plot the numerical solutions and long-wave asymptotics, respectively.

'no-flux' boundary condition at the surface $\psi = 0$ implies $\tan\alpha(z = 0) = \infty$ which it is convenient to present as

$$\cos(\alpha(z = 0; c)) = 0. \tag{5.5}$$

The equation (5.5) has been solved with respect to c. The results of the computations are presented in figure 5.

It is easy to see that for all profiles the pole tends fast to its asymptotic position as k decreases. Note, that the asymptotics work reasonably well up to moderate values of k, especially for the Blasius flow.

An alternative view of the behaviour of $c_p(k)$ yields a picture of the trajectories of the pole on the c-plane with k varying from 0 to ∞ presented in figure 6. The trajectories have similar shape but differ somewhat in parameters. The pole trajectories for all flows start at $k = 0$ at the point $c = U_s$ and as k grows form a loop. The loop differs in size and slightly in shape for the different profiles, however, all trajectories tend to the same initial point $c = U_s$ when k tends to infinity. At certain k (different for different flows), the pole intersects the cut drawn from the point U_s, then residue at the pole loses any physical sense. However, well before the intersection, the pole acquires an essential negative imaginary part and may not be taken into account in evolutionary problems because of strong decay of the relevant wavenumbers. Nevertheless, we stress that the absolute value of $\operatorname{Im} c_p(k)$ does not grow infinitely as our asymptotics suggest, but is bounded from above by a finite value.

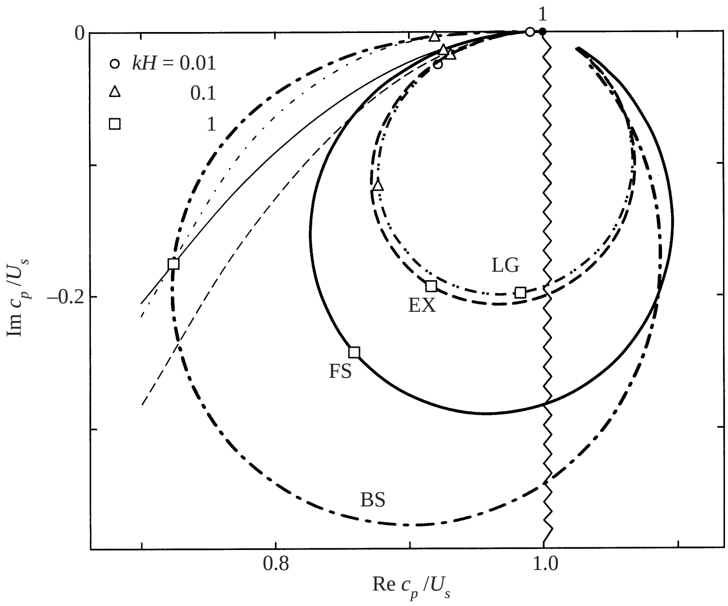

FIGURE 6. Trajectories of the pole $c_p(k)$ on the c-plane for various flows. (Notation as in figure 5. Teeth-like line indicates the vertical cut from the point $c = U_s$.)

Discussion

The results of the computations summarized above in figures 5 and 6 enable us to make a number of important conclusions. First, it was found that the analytical asymptotics work quite well for small to moderate k. Secondly, we traced the pole position beyond the small k range. The question as to whether the quasi-modes linked to the pole are of importance in the evolutionary problems is almost entirely determined by the decay rate $|\mathrm{Im}\, c_p(k)k|$. In the generic situation, the decay rate sharply increases with k and, therefore, only the range of small k covered by the analytical asymptotics should be taken into account. Thus, the long-wave asymptotics describe the evolution of a wide class of initial perturbations, not necessarily the long-wave ones. (Evolutionary problems for non-monochromatic initial perturbations with broad spectra are considered in detail in the subsequent Part 2.) This fact provides an *a posteriori* justification of our analytical approach.

For some specific profiles the decay rate $|\mathrm{Im}\, c_p(k)|$ might prove to be very small even in the range of intermediate k, i.e. $k \sim O(1)$. Since $|\mathrm{Im}\, c_p(k)|$ is roughly proportional to U_r'', then for a flow having a segment of low curvature in the profile, the pole can 'float up' for intermediate k. Such flows require a special consideration which goes beyond the scope of the present work focused on the generic situations only.

5.2. *Direct numerical simulation of the initial problem*

To check the predictions of the asymptotic theory for the evolutionary problem the only way is to apply direct numerical simulation. Since the direct simulations are time-expensive, we confined ourselves to consideration of one particular basic flow profile and one shape of initial perturbation. The initial value problem (2.4) has been solved numerically for a set of different wavenumbers for the FS-profile and a Gaussian initial vorticity distribution

$$\omega_0 = \exp\{-z^2\}. \tag{5.6}$$

The pseudospectral method is applied, based on the Chebyshev polynomials expansion with respect to z (Canuto *et al.* 1987). For integration with respect to time, the Runge–Kutta method with controlled time step is used.

We trace the evolution of the energy density of the initial Gaussian perturbation for a number of different and not necessarily small k and compare the outcome with the predictions of our asymptotic theory.

First, we write down the explicit expressions for the initial velocity field and energy for small k

$$w_0 \approx -\tfrac{1}{2}\mathrm{i}k[1-\exp(-z^2)+\sqrt{\pi}z\,\mathrm{erfc}(z)]+O(k^2), \tag{5.7a}$$

$$u_0 \approx \tfrac{1}{2}\sqrt{\pi}\,\mathrm{erfc}(z)+O(k), \tag{5.7b}$$

$$E(0) \approx \frac{1}{4}\frac{\pi}{4}0.33+O(k) \simeq 0.0649+O(k). \tag{5.7c}$$

Thus, $w_0(z\sim 1)\approx -\tfrac{1}{2}\mathrm{i}k$.

Then we single out the contribution of the pole at the initial moment, taking into account that for the chosen initial vorticity $\int_0^\infty \omega_0\,\mathrm{d}z = \tfrac{1}{2}\sqrt{\pi}$:

$$w_p \approx -\tfrac{1}{2}\mathrm{i}k\sqrt{\pi}(1-U_z), \tag{5.8a}$$

$$u_p \approx \tfrac{1}{2}\sqrt{\pi}U_z', \tag{5.8b}$$

$$E_p \approx \frac{1}{4}\frac{\pi}{4}0.33. \tag{5.8c}$$

In the long-wave approximations the quasi-mode energy obviously decays as $\exp(-2c_\mathrm{i}kt)$. The results of the comparisons with the direct computations are summarized in figure 7, where plots of the disturbance energy evolution $E(t)$ are presented in logarithmic scale for four different k.

The plots clearly show excellent agreement with the asymptotic theory for k up to $O\,10^{-1}$. For moderate k, say $k\approx 0.3-0.4$, the analytic formulae proved to be helpful for a qualitative description.

6. Discussion

We begin with a brief summary of the main results and then discuss their implications in a wider context.

6.1. *Conclusions*

We have solved Cauchy's problem for the spatially monochromatic smooth initial perturbation of a boundary-layer-type flow without inflection points. A rich variety of interesting cases is found to be possible; however, we focus our attention exclusively on the generic situation. We have shown that a generic initial perturbation evolves according to a universal scenario, provided its wavelength is long compared to the boundary-layer thickness. First, there is a relatively short initial transition period, when the 'phase mixing' of continuous spectrum harmonics of initial perturbation takes place and there is no universal asymptotics. In this period the perturbation amplitude can increase or decrease, remaining of the same order in ϵ. Then follows a long time interval dominated by the quasi-mode, where the velocity field perturbation behaves as if it were indeed a single discrete spectrum mode. The mode is weakly decaying as $\exp(-\epsilon^3 t)$. The final stage of evolution occurs after the eventual decay of the quasi-mode: the perturbation velocity field can no longer be characterized by any

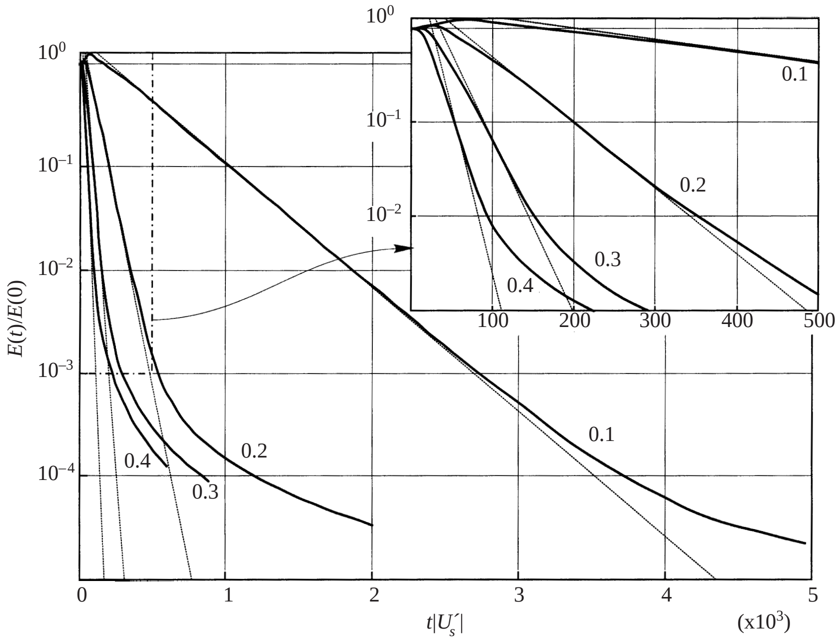

FIGURE 7. Evolution of the disturbance energy $E(t)$ for $kH = 0.1, 0.2, 03$ and 0.4. Solid lines and dashed lines show, respectively, the results of the direct simulations and the analytical theory. A scaled fragment of the plot is shown separately in the frame.

certain vertical structure, although the field amplitude decay does obey the universal t^{-2} law as $t \to \infty$. We found explicit analytic formulae both for the time interval and the degree of the quasi-mode dominance (see (4.19), (4.21), (4.20), (4.22)). Direct numerical simulation confirmed the analytically found scenario of field evolution outlined above (see figure 7).

We recall that from the mathematical viewpoint the quasi-mode understood as a solution due to the residue in the Landau pole is not a true discrete mode of the problem since it contains a velocity jump in the critical layer (4.4) and therefore does not satisfy the Rayleigh equation at this point. We have shown that for the flows under consideration these jumps are very small, and therefore the quasi-mode has no singularities in the velocity field to the leading order. This makes the quasi-modes a practical tool of investigation. We stress that the solution of the evolutionary problem remains always smooth since the critical layer jump is compensated by that of the non-modal part of the solution. We have shown that the Landau damping is asymptotically small for long-wave perturbations but sharply increases with k; this implies that long-wave components should prevail at large time for almost arbitrary, not necessarily long-wave, perturbations. We conclude that the results provide a solid mathematical foundation for applying the quasi-mode concept to boundary-layer type shear flows.

6.2. *Some implications*

6.2.1. *Piecewise linear approximations and method of contour dynamics*

The concept of quasi-modes sheds new light on the foundations of one of the widely used methods in hydrodynamics, the so-called *piecewise linear approximation*. The method was first introduced probably by Rayleigh (1892), and then flourished

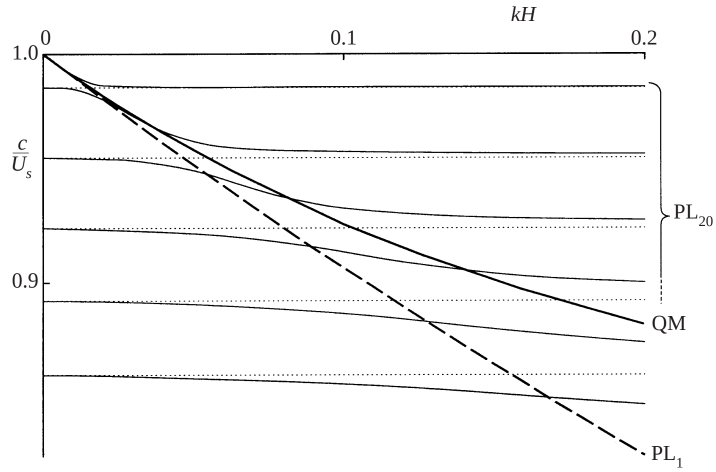

FIGURE 8. Dispersion curves $c(k)$ for the FS flow. The bold line shows the real part of $c(k)$ for the quasi-mode. The dashed bold line shows $c(k)$ for the piecewise linear approximation with one break PL_1. Thin solid lines depict phase velocities of some of 20 modes $c_n(k)$ within the framework of the 20-break model PL_{20}. Thin dotted lines indicate the positions of the breaks.

in the computer era. The great gain in simplicity is achieved by approximating the real smooth velocity profiles by piecewise linear ones (that is representing the flow as a set of the constant vorticity layers). Notice that the overwhelming part of the linear and especially nonlinear problems solved for atmosphere and ocean flows is based just on this approximation (e.g. Gossard & Hooke 1975; Pedlosky 1982). In the context of linear and weakly nonlinear problems the required solutions in each layer are expressed via elementary functions. The method of contour dynamics (e.g. Pullin 1991), often used for simulations of two-dimensional flows, is a strongly nonlinear generalization of the piecewise linear approach, the flow is split into regions of constant vorticity and the system of equations describing the dynamics of their boundaries is solved numerically.

In spite of the long history and wide use of the method, a number of fundamental questions have not yet been satisfactorily answered. We list just a few: Why and when does this method work?; How many breaks should be taken?; When is the solution structurally stable with respect to the profile smoothing?; How many modes do really exist in the original smooth profile flow, if the number of modes in its piecewise linear approximation is equal to the number of breaks specified by the order of approximation? The quasi-mode concept enables us to address, at least partially, these questions.

First consider how well piecewise linear approximations with different numbers of breaks describe spectral properties of a shear flow taking FS-flow (5.2) as a characteristic example. We will refer to an N-break approximation as a PL_N approximation. In figure 8, dispersion curves are plotted for the FS-flow for the real part of the quasi-eigen mode, for a one-break approximation and for a 20-break approximation.

We have earlier established that the quasi-mode dispersion law found in § 3.3 adequately describes spectral properties of the dominant perturbation of the flow. We can easily see from figure 8 that the PL_1 approximation qualitatively (and quantitatively for long wave $kH \lesssim 0.1$) provides $c(k)$ close to that of the quasi-mode. At the same time, we have 20 dispersion curves for the PL_{20} model and none of them describes adequately the true dispersion. Note, that the phase velocity of every mode varies gradually in the limits of velocities of the particular layer ($[U_{n-1}, U_n]$) and large parts of these curves are horizontal and close to the velocities in the breaks U_n ($n = 1, \ldots, N$). The dispersion curves provided by the PL_{20} model are similar to the plots of split frequencies for oscillators with two degrees of freedom. Non-horizontal parts of two modes approximately describe the true dispersion in certain narrow intervals in k.

Thus, in the context of spectral properties, the conclusion is that only the one-break model is adequate. Although its applicability is confined to long-wave perturbations, this is the range that matters in evolutionary problems.

Now we test the ability of various models to describe evolution of an initial perturbation. Let the initial disturbance be prescribed by (5.6). Within the framework of the PL_N model we, in principle, can describe any smooth perturbation; however, it is strongly preferable to deal with perturbations that can be created entirely by distortion of the interfaces between the layers. Then the vorticity of the layer is conserved, and the strong nonlinear generalization, including the contour dynamics method seems to be straightforward. Such a perturbation can be presented as a sum of discret spectrum (DS) modes only. In the opposite case, the additional vorticity should be inserted into the flow and when solving a nonlinear evolution problem we have to consider the continuous spectrum (CS) modes and their interaction with DS-modes as well. However, if, as most other authors do, we take the first option, i.e. consider a perturbation composed entirely of the DS-modes, we cannot satisfy exactly arbitrary initial conditions, for example (5.6). We take the best approximation to this initial perturbation in the following sense

$$\int_0^{+\infty} |w_{0,\mathrm{PL}_N}(z) - w_0(z)|^2 + |u_{0,\mathrm{PL}_N}(z) - u_0(z)|^2 \,\mathrm{d}z \rightarrow \min.$$

Eventually, upon having specified the initial condition in terms of an N-break approximation, we simulate the field evolution by direct integration of the corresponding set of ODEs. Choosing again the field energy as the most representative parameter, we plot in figure 9 the resulting energy evolution with time for the case $kH = 0.2$ and different numbers of breaks. We can see that the PL_2–PL_5 models do not describe the evolution of the perturbation energy. The PL_{20} model describes well at least an initial part of the intermediate asymptotics, while the PL_{100} model is able to describe this asymptotics regime almost completely, giving, however, a qualitatively wrong prediction for larger times: the perturbation grows rather than decreases. Only the PL_{300} model is able to describe satisfactorily all the stages of the evolution, although at the later stages the discrepancy increases and becomes apparent. Moreover, it is worth noting that PL_{300} works so well only due to a specially optimized set of breaks approximating the basic profile (the density of the break distribution increases towards the surface), otherwise, the curves would diverge much earlier or it would require many more breaks to obtain the same results.

Notice that the PL_1 model gives constant energy and hence, at first sight, cannot be a satisfactory model in this sense. Nevertheless, if we approximate the profile by a piecewise linear function with one break (see figure 1a) and make use of the well-known dispersion of the mode for sufficiently small kH, this enables us to determine the position of its critical layer and then eventually find the decay rate of this mode due to the Landau damping (e.g. Landau 1946; Briggs *et al.* 1970; Rabinovich & Trubetstkov 1991)

$$c_i \approx -\pi k^2 H^4 U_s''.$$

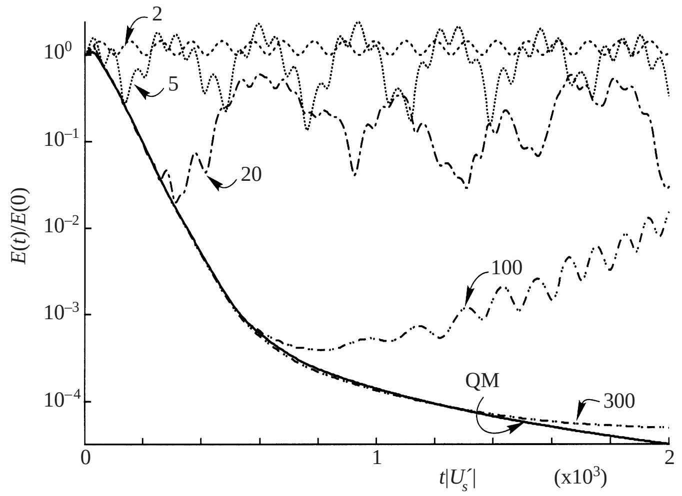

FIGURE 9. $E(t)$ for various PL_N models compared to the pseudospectral simulations for the FS flow. The solid line shows the benchmark pseudospectral simulation for $KH = 0.2$. Dotted lines depict $E(t)$ given by the different piecewise linear models (the corresponding number n of modes is indicated above each curve). The dashed line distinguishes predictions of the 300-break model.

Then the single mode, with this correction prompted by the acquired understanding of quasi-modes taken into account, describes satisfactorily the evolution and dispersion of the eigen-mode of the flow.

In this sense, contrary to common opinion 'the more the better', one break proves to be much better than several: it does not add extra modes, it describes the dispersion reasonably well and, after a simple correction, the attenuation. Several breaks describe everything quite badly. The models with very large number of breaks N tend to describe the evolution rather well, provided N is large enough; however, for this case DS-modes in PL_N profile play the role of CS modes in the smooth profile.

Although the comparison was carried out for a single profile of shear flow without inflection points, nevertheless the acquired understanding enables us to suggest what might be the recipe for untested yet more complicated situations, where there is more than one DS or quasi-mode. We expect that the number of breaks in the best piecewise linear approximation for a generic situation should be either very small and equal to the number of quasi- and DS-modes, and then each break mode would reflect a certain physical reality, or tend to infinity. In the latter case DS-modes in such a model would mimic CS-modes. Turning to the contour dynamics method we note that the method is usually applied for strongly nonlinear situations, where neglected CS-modes 'filtered out' by the N-mode approximation of the initial distribution are expected to prove essential. This implies that there is no room for small N models and only by employing very large N approximations, where DS-modes can substitute CS spectrum, we can expect a good description of strongly nonlinear processes. This conclusion is in agreement with the results of simulations by Legras & Dritschel (1993).

6.2.2. *The next steps and beyond*

The present work was confined to the initial problem for two-dimensional monochromatic inviscid perturbations of boundary-layer-type shear flows. In work underway we extend our analysis in the following directions.

Viscosity: we show that the quasi-mode is structurally stable with respect to introducing small viscosity, i.e. that the quasi-mode turns into the corresponding true mode of the Orr–Sommerfeld equation.

Broad spatial spectrum: we show that quasi-mode is the true asymptotics for perturbations with broad spatial spectrum, rather than an intermediate asymptotics as it is the case for the spatially harmonic perturbations. Three-dimensional perturbations of two-dimensional flows and the range of validity of their linear description due to accumulation of nonlinear effects will be also considered.

Although the implications of the essentially linear concept for nonlinear and especially weakly nonlinear problems are numerous, they can be grouped along a few major lines.

For intrinsic dynamics of generic inviscid shear flows it would be impossible to develop a weakly nonlinear description since there is a fundamental problem. Not only has one to consider a continuum of the continuous spectrum modes to describe any smooth perturbation, these modes, because of their singularity, do not admit a weakly nonlinear description. Employing the quasi-mode concept one circumvents this problem at least for boundary-layer flows as the quasi-mode has no singularities to the leading order. This allows one to develop models able to describe transition from the linear to the nonlinear regime and, in particular, the formation and dynamics of solitons (Shrira 1989; Shrira & Voronovich 1996).

The quasi-mode concept is instrumental in understanding the interaction of boundary layers with waves of a different nature when they are present in the system (e.g. the interaction of internal gravity waves in the ocean with surface or bottom boundary layers (Voronovich *et al.* 1998*a*, *b*), the interaction with gravity waves in free surface flows subject to gravity, etc.). In particular, it became possible to advance in describing a nonlinear critical layer for a wideband wavepacket by formulating the problem in terms of wave–wave interaction, rather than a wave–current one (Voronovich *et al.* 1998*b*). Often, quasi-modes can participate in a regular manner in nonlinear resonant interactions with other modes, forming triads, quartets, cascades, etc.

The study of small perturbation dynamics in shear flows is traditionally linked with the flow stability aspect and is aimed at understanding of laminar–turbulent transition. In the quasi-mode line of thought we are aware of two basic nonlinear mechanisms by virtue of which the presence of a weakly decaying quasi-mode can lead to instability. The first one is probably responsible for the laminar–turbulent transition in wind-driven free-surface shear flows: quasi-mode solitary waves emerge with time from a finite-amplitude initial perturbation, then a strong self-focusing-type transverse instability leads to wave blow-up (Pelinovsky & Shrira 1995; Shrira *et al.* 2002). It can be viewed as a particular case of secondary instability. The second scenario is based on nonlinear resonant interaction of a quasi-mode with true modes of different origin, e.g. quasi-modes in either wind or water boundary layers at an air/water interface can form explosive resonant triads with the surface gravity–capillary waves (Voronovich & Rybak 1978; Romanova & Shrira 1988). Such triads tend to blow up even in the absence of linear instability. Although these cases of explosive instability were found within the framework of simple piecewise-linear models, use of the QM-concept is essential in judging the relevance of such cases to reality. Taking into account the decay rate typical of the quasi-modes results in a certain amplitude threshold of instability which has to be estimated to judge the importance of the process. (One should, however, be very cautious carrying out such estimates since even small nonlinearity can change drastically the decay rate of the quasi-modes and even turn it into zero.) Whether these two mechanisms of nonlinear instability exhaust the list and where other situations of physical interest with such instabilities lie remains an intriguing open question.

It is also worth noting, that for flows without linearly unstable modes (or with very weak instabilities) an alternative approach to laminar–turbulent transition due to the so-called 'non-modal' or 'transient' growth has recently received considerable attention (e.g. Schmidt & Henningson 2001). The approach is based on the idea that within the framework of linearized stability problems described by non-normal operators, a transient amplification of primordial noise up to significant levels might occur, thus providing an apparent instability. Although the quasi-modes appear in the linearized stability problems, also described by non-normal operators, the phenomenon of quasi-modes and the above mentioned mechanisms of quasi-mode-based instabilities are not directly related to the specific pseudospectra properties essential for significant growth (Trefethen, Trefethen & Reddy 1993; Schmidt & Henningson 2001). The point we would like to stress here is that not only are these phenomena not directly related, but they unfold on different timescales, the transient growth normally precedes the emergence of the quasi-mode (see, for example, the curve corresponding to $kH = 0.1$ in the box in figure 7, where a non-spectacular transient growth is discernable for small t (for a significant transient growth the presence of transverse spatial dimension is essential).

The authors are grateful to M. J. A. O'Callaghan for the helpful comments on the first draft of the paper and to an anonymous referee for the key references and helpful comments. The work was supported by Forbairt Basic Research Grant SC-98-530 and by INTAS (Grant 97-575).

Appendix A. The Green's function in the long-wave approximation

A.1. *The Green's function via particular solutions of the Rayleigh equation*

In this Appendix we present the derivation of the Green's function specified by equation (2.12) with the boundary conditions (2.4*b, c*). As we mentioned, the left-hand side of (2.12) is the Rayleigh equation for small harmonic disturbances $\psi \propto \exp[\mathrm{i}k(x-ct)]$ with phase velocity c:

$$(\partial_z^2 - k^2)\psi - \frac{U''}{U-c}\psi = 0. \tag{A 1}$$

Let ψ_1 and ψ_2 be particular solutions of this equation, ψ_1 satisfying the surface condition (2.4*b*), ψ_2 satisfying the condition at the infinity (2.4*c*). Then the Green's function can be represented in the form

$$\tilde{G}(z|h;c) = \begin{cases} -\dfrac{\psi_1(z)\psi_2(h)}{\mathrm{i}kV_hW} & (z \leqslant h), \\ -\dfrac{\psi_1(h)\psi_2(z)}{\mathrm{i}kV_hW} & (z \geqslant h), \end{cases} \tag{A 2}$$

Here, $W = \psi_1'\psi_2 - \psi_2'\psi_1$ is the Wronskian independent of z.

Thus, the problem reduces to solving the Rayleigh equation. The peculiarity lies in the fact that, in the present context, c belongs to the integration contour Γ, i.e. it has a significant positive imaginary part, and, therefore, there are no singularities of solution of the Rayleigh equation.

To obtain the particular solutions ψ_1 and ψ_2, two different long-wave expansions prove to be required.

A.2. *Solution vanishing at the surface. The Heisenberg-type expansion*

To proceed, we first cast the Rayleigh equation into the following vector form:

$$\boldsymbol{y}' = k\boldsymbol{A}\boldsymbol{y}, \quad \boldsymbol{y} = \begin{bmatrix} \psi/V_z \\ (\psi' V_z - \psi V_z')/k \end{bmatrix}, \quad \boldsymbol{A} = \begin{bmatrix} 0 & V_z^{-2} \\ V_z^2 & 0 \end{bmatrix}.$$

It is easy to check that if a vector $\boldsymbol{y}$ is given in the point z_0 then the solution at any point z can be found using a matrix $\boldsymbol{F}$ independent of the initial conditions for $\boldsymbol{y}$, satisfying the matrix ordinary differential equation and equal to the identity matrix in z_0:

$$\boldsymbol{y}(z) = \boldsymbol{F}(z_0|z)\boldsymbol{y}(z_0), \tag{A 3a}$$

$$\boldsymbol{F}' = k\boldsymbol{A}\,\boldsymbol{F}, \tag{A 3b}$$

$$\boldsymbol{F}(z_0|z_0) = \boldsymbol{I} \equiv \begin{bmatrix} 1 & 0 \\ 0 & 1 \end{bmatrix}. \tag{A 3c}$$

The following properties of the matrix $\boldsymbol{F}$ must be noted:

(i) $\det \boldsymbol{F}(z_0|z) \equiv 1$;

(ii) $\boldsymbol{F}(z_0|z) = \boldsymbol{F}(z_0|z_1)\boldsymbol{F}(z_1|z)$;

(iii) $\boldsymbol{F}(z|z_0) = \boldsymbol{F}^{-1}(z_0|z) = \begin{bmatrix} F_{22}(z_0|z) & -F_{21}(z_0|z) \\ -F_{12}(z_0|z) & F_{11}(z_0|z) \end{bmatrix}$;

(iv) $\boldsymbol{F}(0|z) = \begin{bmatrix} \cosh kz & V_z^{-2}\sinh kz \\ V_z^2 \sinh kz & \cosh kz \end{bmatrix}$ if $V_z \equiv \text{const}$.

Relations (A 3b, c) can be written as an integral matrix equation

$$\boldsymbol{F}(z_0|z) = \boldsymbol{I} + k\int_{z_0}^{z} \boldsymbol{A}(z')\,\boldsymbol{F}(z_0|z')\,\mathrm{d}z' \tag{A 4}$$

that admits subsequent iterations for small k (in fact, we are employing the smallness of $\epsilon = kH$, but it is convenient at this stage to keep the dimensional variables):

$$\boldsymbol{F} = \boldsymbol{I} + k\boldsymbol{F}_1 + k^2\boldsymbol{F}_2 + \cdots. \tag{A 5}$$

It is possible to show that this series converges absolutely but not uniformly in z for infinite interval $z \in [0, +\infty)$. Here we do not use the absolute convergence. An example of the non-uniformity is most easily seen in the case of z-independent flow.

To order k, the long-wave approximation of the matrix $\boldsymbol{F}$ for an arbitrary flow takes the form:

$$\boldsymbol{F} = \begin{bmatrix} 1 & k\displaystyle\int_{z_0}^{z} V_h^{-2}\,\mathrm{d}h \\ k\displaystyle\int_{z_0}^{z} V_h^2\,\mathrm{d}h & 1 \end{bmatrix} + O(k^2). \tag{A 6}$$

The solution ψ_1, that we are looking for, can then be presented via two components of the matrix $\boldsymbol{F}$

$$\psi_1(z) = V_z F_{12}(0|z) \tag{A 7a}$$

$$\psi_1'(z) = V_z' F_{12}(0|z) + kV_z^{-1}F_{22}(0|z). \tag{A 7b}$$

A.3. *Solution decaying at infinity. Miles's approximation*

As the expansion (A 5) does not converge uniformly (the greater z, the more terms of the series are necessary for a satisfactory approximation), we cannot apply it to obtain the second particular solution ψ_2 decaying at infinity. We use here another expansion. The latter, however, is not convenient for describing the solutions vanishing at the surface. We look for the decaying solution in the form

$$\psi_2 = \exp\left[\int_0^z f(z_1)\,\mathrm{d}z_1\right], \tag{A 8}$$

where $f(z) = \psi'/\psi$ is the function satisfying the Riccati equation

$$f' + f^2 = k^2 + \frac{V_z''}{V_z}, \tag{A 9}$$

obtained after substitution of (A 8) into (A 1). The boundary condition for f specified by (2.4c) is

$$f(z \to +\infty) \to -k.$$

Equation (A 9) admits uniform expansion for $z \in [0, +\infty)$. Actually, if we seek the solution in the form $f = f_0 + kV_\infty^2 V_z^{-2} g$ we find for $k = 0$: $f_0 = V_z'/V_z$. Then we find that the auxiliary function g satisfies the equation (function g coincides within factor $-k$ with the function Ω introduced by Miles (1957) for similar purposes)

$$g' = k\left[\frac{V_z^2}{V_\infty^2} - g^2\frac{V_\infty^2}{V_z^2}\right], \tag{A 10}$$

(compare with (A 3b)) and the condition

$$g(z \to +\infty) \to -1. \tag{A 11}$$

Equation (A 10) and condition (A 11) can be united into an integral equation

$$g = -1 + k\int_\infty^z \left[\frac{V_h^2}{V_\infty^2} - g^2\frac{V_\infty^2}{V_h^2}\right]\mathrm{d}h, \tag{A 12}$$

(compare with (A 4)) which admits the subsequent approximations with respect to small k for the limited (i.e. $V_\infty \neq \pm\infty, V_s \neq \pm\infty$) flows:

$$g = g_0 + kg_1 + \cdots,$$

$$g_0 = -1, \quad g_1 = \int_\infty^z \left[\frac{V_h^2}{V_\infty^2} - \frac{V_\infty^2}{V_h^2}\right]\mathrm{d}h, \ldots .$$

Function g_1 and the higher-order functions g_n decay as $z \to \infty$ and are bounded if $c \in \Gamma$. This proves uniform convergence.

Finally, we present the solution ψ_2 and its derivative as

$$\psi_2(z) = V_z\,E(0|z), \tag{A 13a}$$

$$\psi_2'(z) = \left[V' - k\,V_\infty^2 V_z^{-1} - k^2 V_\infty^2 V_z^{-1}\chi\right]\,E(0|z), \tag{A 13b}$$

$$E(0|z) = \exp\left\{-k\,V_\infty^2\int_0^z V_h^{-2}\,\mathrm{d}h - k^2 V_\infty^2\int_0^z V_h^{-2}\chi\,\mathrm{d}h\right\}, \tag{A 13c}$$

$$\chi(z) = k^{-1}(g+1) = O(k^0). \tag{A 13d}$$

A.4. *Green's function in terms of the matrix* $\mathbf{F}$ *and the decaying solution*

The Wronskian of the derived solutions (A 7) and (A 13) is

$$W = kE(0|z)[F_{22}(0|z) + V_\infty^2 F_{12}(0|z)(1 + k\chi(z))]. \tag{A 14}$$

As the exact Wronskian does not depend on z, we can substitute instead of z any value, say B. Since the accuracy of the solutions ψ_1 and ψ_2 is not uniform in z and is decreasing for very large and very small small z, respectively, it is appropriate to choose B to be $O(1)$, where both ψ_1 and ψ_2 have good accuracy. Thus, we assume: $kB \ll 1$, $B/H \gg kH$. B is a fictitious, auxiliary parameter and, as we show below, any dependence on B drops out from the final formulae, meanwhile we keep it for our intermediate manipulations.

Substituting (A 7) and (A 13) into (A 2) we obtain the Green's function in the form

$$\mathrm{i}k\tilde{G} = \begin{cases} \dfrac{-V_z F_{12}(0|z)\, E(B|h)}{k[F_{22}(0|B) + V_\infty^2 F_{12}(0|B)(1+k\chi(B))]}, & z \leqslant h \\ \dfrac{-V_z F_{12}(0|h)\, E(B|z)}{k[F_{22}(0|B) + V_\infty^2 F_{12}(0|B)(1+k\chi(B))]}, & z \geqslant h, \end{cases} \tag{A 15}$$

where B is a point where the Wronskian is calculated.

In this approximation we substitute functions F_{21}, F_{22}, E by their expansions

$$F_{12}(0|z) = kI_z + O(k^3), \tag{A 16a}$$

$$F_{22}(0|z) = 1 + O(k^2), \tag{A 16b}$$

$$E(B|z) = 1 - kV_\infty^2(I_z - I_B) + O(k^2), \tag{A 16c}$$

and neglect the auxiliary function χ specified by (A 13*d*) which enters into $O(k^2)$ terms only.

Then the Green's function takes the following approximate form:

$$\mathrm{i}k\tilde{G} \cong \begin{cases} \dfrac{-V_z I_z\,[1 + kV_\infty^2(I_B - I_h)]}{1 + kV_\infty^2 I_B}, & z \leqslant h \\ \dfrac{-V_z I_h[1 + kV_\infty^2(I_B - I_z)]}{1 + kV_\infty^2 I_B}, & z \geqslant h, \end{cases} \tag{A 17}$$

which can be rewritten in a more compact and convenient form (3.1).

A few remarks seems to be helpful in elucidating the approximations and compromises resulted in the compactness of the presentation (A 17), (3.1).

We are primarily interested in the evolution of the field components u, v and ω given by a convolution of the Green's function and the initial vorticity ω_0 localized in the layer $z \lesssim H$ (see § 2.3). We recall that our expansion in k is not uniform in z, h; however we can tolerate considerable deviations of the derived expressions (A 17) as function of z and h from the exact Green's function, as long as these deviations do not contribute to the convolution in the main order. In particular, we can allow a large deviation in a very narrow domain. Say, owing to poor convergence of ψ_2 for small z the discrepancy between the found and exact Green's functions is not small, but it can be shown that its contribution in the convolution is negligible. The fact that ω_0 is effectively zero outside the boundary layer $z \lesssim H$ enables us to relax somewhat our requirements on the Green's function behaviour for large z (strictly speaking the Green's function must satisfy (2.4*c*)). Its deviation in the large-z asymptotics results from the poor convergency of ψ_1 at large z. We can safely ignore the discrepancy for the solution within the boundary layer: $z, h \lesssim H$. Outside the boundary layer this discrepancy results in unphysical behaviour of some field components: w does not decay when $z \to \infty$ (see (4.7)). The proper large-z asymptotics can be obtained by applying the multiple scale technique, i.e. by considering an expansion in k assuming in each order the functions to be dependent on two independent variables z and

$\zeta \equiv (kH)z$. This kind of procedure was carried out in Shrira (1989). For the problem under consideration the procedure would have resulted merely in an exponential factor $\exp(-kz)$ which is of importance for large z for only one field component: vertical velocity w (other field components, being localized within the layer, are unaffected by this factor). However, since our main interest is in the processes within the boundary layer, we did not find the use of a more sophisticated procedure justified. We stress that the main results of the paper do not depend on the presence or absence of this factor. Only large-z asymptotics of w is affected, but w is playing little role in the field dynamics. However, to preserve the physical adequacy of the solution for w in the whole domain we merely inserted the exponential factor $\exp(-kz)$ in (4.7). Comparison with the 'exact' numerical solution shows that such a crude amendment describes well all vertical dependences over the whole domain.

Appendix B. Contributions of the Green's function singularities

Here, we present the detailed analysis of the contributions due to the singularities U_z, U_s and U_h of the Green's function listed in table 1. We begin with the singularity U_s as the simplest one.

B.1. *Contribution of the point $c = U_s$*

In the vicinity of the point $c = U_s$, the leading term of the asymptotics is

$$G_s = \frac{k}{2\pi}\frac{U_s'' V_{sz}}{k^2 U_s' \Delta U^4}\int_{\Gamma_s} V_s^2 \log V_s \exp(-\mathrm{i}kct)\,\mathrm{d}c,$$

where $V_{sz} = U_s - U_z$. Taking into account the fact that the branches of the logarithmic functions at the opposite sides of the cut differ by the term $2\pi\mathrm{i}$, we can take it explicitly:

$$G_s = \frac{k}{2\pi}\frac{U_s'' V_{sz}}{k^2 U_s' \Delta U^4}\int_{U_s}^{U_s+\mathrm{i}\infty} V_s^2 (2\pi\mathrm{i}) \exp(-\mathrm{i}kct)\,\mathrm{d}c = -\frac{2U_s'' V_{sz}}{k^4 t^3 U_s' \Delta U^4}\exp(-\mathrm{i}kU_s t). \quad \text{(B 1)}$$

To evaluate the characteristic time when these asymptotics are valid we similarly find the next term in the expansion in V_s, that is

$$\tilde{G}_s^{(1)} = \frac{2\mathrm{i}V_z (U_s'')^2}{k^2 (U_s')^3 \Delta U^4} V_s^3 \log^2 V_s \;\Rightarrow\; G_s^{(1)} \sim \frac{(U_s'')^2 V_{sz}}{k^5 t^4 (U_s')^3 \Delta U^4}\log(U_s' t)\exp(-\mathrm{i}kU_s t). \quad \text{(B 2)}$$

Comparing (B 1) and (B 2), we find that they become of the same order at $t = t_s$ given by (4.16). Finally, calculating the convolution of G_s with the initial disturbance ω_0 we find the contribution of this singularity to velocity and vorticity components given by (4.15).

B.2. *Contribution of the point $c = U_z$*

The leading term of the Green's function $\tilde{G}$ in the vicinity of the point $c = U_z$ for $z \gg z_r$, where $U(z_r) = \operatorname{Re} c$, takes the form

$$\tilde{G}_z = \frac{U_z''}{\mathrm{i}k(U_z')^3} V_z \log V_z\, \theta(h - z),$$

where $\theta(z)$ is the Heaviside unit-step function. Performing integration similar to the previous case, we obtain

$$G_z \simeq \frac{U_z''}{k^2 t^2 (U_z')^3}\exp(-\mathrm{i}kU_z t)\theta(h - z). \quad \text{(B 3)}$$

To evaluate the characteristic time when these asymptotics become valid we have to consider the next term in the expansion of $F_{21}(0|z)$ with respect to k, which yields

$$\tilde{G}_z^{(1)} \simeq \frac{F_z k^2 U_z''}{6\mathrm{i}(U_z')^5} V_z^3 \log V_z\, \theta(h-z) \quad \Rightarrow \quad G_z^{(1)} \simeq \frac{F_z U_s''}{\mathrm{i}k^2 t^4 (U_s')^5} \exp(-\mathrm{i}kU_z t)\, \theta(h-z). \quad \text{(B 4)}$$

Comparing (B 3) and (B 4), we find that the characteristic time t_z is (4.10) that is much smaller than t_s.

If $z \sim z_r$, the second term in (4.1) becomes essential (see table 1). In the case $h \gg z_r$, we can approximate integral $I_h(U_z)$ by its leading term $(V_s U_s')^{-1}$ (see (3.3)). Changing the variables $\sigma(c) = \mathrm{i}(c - U_z)$, we reduce the inverse Laplace transform to the integral:

$$G_z^a = \frac{-2\pi \mathrm{i} U_r'' \Delta U^2}{U_s'^4} \exp(-\mathrm{i}ktU_z) \int_0^{+\infty} \frac{\sigma\, \mathrm{d}\sigma}{\sigma + \mathrm{i}(U_z - c_p)} \exp(-kt\sigma),$$

which can be taken in the explicit form via the integral exponent function:

$$G_z^a \simeq \frac{\Delta U^2 U_r''}{\mathrm{i}(U_s')^4} \left[\frac{\exp(-\mathrm{i}ktU_z)}{t} - \mathrm{i}k(U_z - c_p)\, E_1[\mathrm{i}kt(U_z - c_p)] \exp(-\mathrm{i}ktc_p) \right] \quad \text{(B 5)}$$

If $h \sim z_r$, the term $-(V_h U_h')^{-1}$ in the approximation for $I_h(U_z)$ becomes essential, so we also have to take into account the pole $(c - U_h)^{-1}$.

Although G_z^a decays more slowly than the leading term (B 4), it does not dominate until $\bar{t} \sim \bar{k}^{-2}$. However, since while finding the convolution, we have to integrate G_z with respect to h, it is possible to show that the contribution of the layer $h \sim z_r$ is small and therefore is neglected throughout our study. It must be taken into account only if the initial vorticity is localized in the layer $z \sim z_r$, a situation interesting for its own merit, but not generic, and hence lying beyond the scope of the present work.

Thus, assuming that the contribution of the layer $h \lesssim z_r$ is small, we finally arrive at the solution for the velocity components and vorticity presented by (4.8)–(4.9).

If t and z satisfy the inequality

$$|kt(U_z - c_p)| \gg 1, \quad \text{(B 6)}$$

we can use the known asymptotics of E_1 for large argument and simplify the formulae for w_z^a and u_z^a:

$$w_z^a \approx \frac{\mathrm{i} U_s'' \Delta U^2}{t^2 (U_s')^4 (U_z - c_p)} \exp(-\mathrm{i}ktU_z) \int_0^\infty \omega_0(h)\, \mathrm{d}h, \quad \text{(B 7)}$$

$$u_z^a \approx \frac{U_s'' \Delta U^2}{t (U_s')^3 (U_z - c_p)} \exp(-\mathrm{i}ktU_z) \int_0^\infty \omega_0(h)\, \mathrm{d}h. \quad \text{(B 8)}$$

Notice that, just in the critical layer, this inequality is valid if $\bar{t} \gg \bar{k}^{-3}$ ($\bar{t} \gg \bar{k}^{-4}$ for the Blasius profile). The term containing function E_1 becomes much smaller than the second term in (4.9).

Summarizing, we have found that the contribution due to the critical layer singularity $c = U_z$ decays as t^{-2} in terms of ψ or w. However, near the critical layer, it decays more slowly for a finite but rather long time. This causes the domination of this solution in the vicinity of the critical layer for sufficiently long time. Solution u_z decays as a whole as t^{-1}, but it also has a slower intermediate decay in the vicinity of the critical layer, and, as a consequence, this part of the solution dominates for sufficiently large time. The velocity component jumps behave differently; they decay exponentially as $\exp\{-kc_i t\}$ (see (4.4)). The vorticity disturbance does not decay at all, but due to the shear becomes more and more oscillating with respect to z, in virtue of the factor $\exp\{-\mathrm{i}U_z kt\}$.

B.3. *Contribution of the point $c = U_h$*

This point contains two singularities simultaneously: the pole and the logarithmic branch point

$$\left\{\frac{1}{V_h}+\frac{U_h''}{(U_h')^2}\log V_h\right\}\left\{\theta(z-h)+\frac{kV_\infty^2}{(c-c_p)}V_s I_z\right\}\frac{V_z}{\mathrm{i}kU_h'}.$$

The residue in the pole V_h^{-1} gives a non-decaying contribution into G_h. Thus, for infinitely large time, the Green's function tends to a harmonic wave representing the continuous spectrum mode $\psi_{CS}(z|h)$ centred at the critical layer $z = h$:

$$G_h(t \to \infty) \to \psi_{CS},$$

$$\psi_{CS} = \frac{1}{U_h'}\left[V_z\theta(z-h) + k\frac{V_\infty^2 V_s}{(c-c_p)}V_z I_z\right]\Bigg|_{c=U_h} \exp(-\mathrm{i}kU_h t).$$

This field is singular and satisfies the Rayleigh equation as a distribution (in the generalized sense). Besides, it satisfies both boundary conditions. The first term in brackets gives the singularity of clear nature: a break for ψ_{CS} (a jump for u_{CS}, the Dirac delta function for ω_{CS}, respectively). If we pull out the singularities from the integral I_z of the second term and retain the singular term with V_z only, choosing the right branch of the logarithmic function, we obtain:

$$\psi_{CS} \simeq \left[\frac{V_z}{U_h'}\theta(z-h) - \frac{kV_\infty^2 V_s}{(c-c_p)}\frac{U_h''}{(U_h')^4}V_z\log|V_z|\right]\Bigg|_{c=U_h} \exp(-\mathrm{i}kU_h t),$$

$$\omega_{CS} \simeq \left[\delta(z-h) - \frac{U_z''}{U_h'}\theta(z-h) - \frac{kV_\infty^2 V_s}{(c-c_p)}\frac{U_h''}{(U_h')^3}\mathscr{P}\frac{U_z''}{V_z}\right]\Bigg|_{c=U_h} \exp(-\mathrm{i}kU_h t).$$

Here, the $\mathscr{P}z^{-1}$ distribution means that the principal value of integral $\int\phi(z)\mathscr{P}z^{-1}\,\mathrm{d}z = PV\int\phi(z)z^{-1}\,\mathrm{d}z$ is taken for any smooth finite function $\phi(z)$.

Note, that the coefficients in the first and second term become of the same order when $h \approx z_r$. Actually, if $h = z_r$ ($U_h = c_r$), then $V_s/(c-c_p)|_{c_r} \approx (U_s - c_r)/(-\mathrm{i}c_i) \approx -\mathrm{i}k^{-1}(U_s')^3\Delta U_\infty^{-2}(U_r'')^{-1}\pi^{-1} = O(k^{-1})$ (or $O(k^{-2})$ for the Blasius profile).

Now we consider the decaying part of the solution (contribution of the $\log V_h$ singularity) and show that we can neglect it in our study. We denote this part by $G_h^{\log}$:

$$G_h^{\log} = \frac{U_h''}{\mathrm{i}k(U_h')^3}\frac{V_{zh}}{t}\theta(z-h)\exp(-\mathrm{i}kU_h t) + G_h^{\log,c_p},$$

$$G_h^{\log,c_p} = \frac{U_h''}{\mathrm{i}k(U_h')^3}\left[\frac{kV_\infty^2}{t}\left(\frac{1}{U_z'} - \frac{1}{U_s'}\right)\exp(-\mathrm{i}kU_h t)\right.$$
$$\left.-\mathrm{i}k^2\left[\left(\frac{c_p}{U_z'} - \frac{c_p}{U_s'}\right) - \left(\frac{U_s}{U_z'} - \frac{U_z}{U_s'}\right)\right]E_1[\mathrm{i}kt(U_h - c_p)]\exp(-\mathrm{i}kc_p t)\right],$$

$$G_h^{\log,c_p} \simeq \frac{U_h''}{\mathrm{i}k(U_h')^3}\frac{kV_\infty^2}{t}\exp(-\mathrm{i}kU_h t)\left[\left(\frac{U_h}{U_z'} - \frac{U_h}{U_s'}\right) - \left(\frac{U_s}{U_z'} - \frac{U_z}{U_s'}\right)\right].$$

The second approximate formula for $G_h^{\log,c_p}$ is valid when the argument of function

E_1 is large. Thus, $G_h^{\log}$ contains a term which does not decay for $\bar{t} < \bar{k}^{-3}$, but it does not exceed $O(\bar{k}^2)$ in terms of ψ_{CS}. The leading term in $G_h^{\log}$ is the first one, but it is also much smaller than ψ_{CS} as $\bar{t} \gtrsim \bar{k}^{-1}$. Finally, we conclude that in our asymptotic study ($\bar{t} \gtrsim \bar{k}^{-1}$) we can suffice with

$$G_h \approx \psi_{CS}.$$

Now we show that a smooth packet of such waves decays with t by analysing the convolution integral

$$\begin{aligned}\psi_h &= \int_0^\infty \psi_{CS}(z|h)\,\omega_0(h)\,\mathrm{d}h \\ &= -\int_0^\infty \left[\frac{V_{zh}}{U_h'}\theta(z-h) + \frac{kV_{zh}I_{zh}}{U_h'}\frac{V_{\infty h}^2 V_{sh}}{(U_h - c_p)}\right]\omega_0(h)\exp(-\mathrm{i}kU_h t)\,\mathrm{d}h,\end{aligned}$$

where $I_{zh} = \int_z^h V_Z^{-2}\,\mathrm{d}Z$.

It is possible to show that for large t the main contribution yields integration in the vicinity of the endpoint $h = 0$ and singular point $h = z$. Our assumption that the initial distribution $\omega_0(h)$ is sufficiently smooth (see (2.2)) is crucial here. We denote the contribution of each point by additional superscripts s or z, respectively: $\psi_h = \psi_{h,s} + \psi_{h,z}$.

To study the contribution of the endpoint $h = 0$, it is useful to employ the first of the alternative formulae for the Green's function (A 17) and assume $h < z$,

$$\mathrm{i}k\tilde{G} = -V_z\,I_h(c)\frac{1 + kV_\infty^2(I_B - I_z)}{1 + kV_\infty^2 I_B}. \tag{B 9}$$

We calculate the residue in the point $c = U_h$, and obtain another representation for ψ_{CS} more suitable for study in the vicinity of U_s:

$$\begin{aligned}\psi_{CS} &= -\frac{V_z}{U_h'}\left.\frac{1 + kV_\infty^2(I_B - I_z)}{1 + kV_\infty^2 I_B}\right|_{c=U_h}\exp(-\mathrm{i}kU_h t) \\ &\approx \left.\frac{V_z}{U_h'}\frac{V_s}{c - c_p}\right|_{c=U_h}\exp(-\mathrm{i}kU_h t).\end{aligned}$$

We could deduce this formula from (3.1), however, this needs more care: we hold terms $O(k^2)$ at the pole, but neglect similar-order terms in the numerator. The advantage of the latter approximation is that we have the explicit factor $V_s(U_h)$ which indicates that $\psi_{CS} \to 0$ as $h \to 0$. Now, we can present $\psi_{h,s}$ as

$$\psi_{h,s} = -\int_0^\infty \left[\frac{V_{zh}}{U_h'}\frac{V_{sh}}{U_h - c_p}\right]\omega_0(h)\exp(-\mathrm{i}kU_h t)\,\mathrm{d}h$$

We change the variable $\sigma(h) = kt(U_s - U_h)$ and obtain an integral in the limits $[0, ktV_{s\infty}]$. Then we expand the integrand into series in t^{-1} taking into account the expansion

$$h = -\frac{\sigma}{ktU_s'} - \frac{\sigma^2}{k^2t^2}\frac{U_s''}{2U_s'^3} + \cdots.$$

As a result, we have

$$\psi_{h,s} = -\exp(-\mathrm{i}kU_s t)\int_0^{ktV_{s\infty}}\left\{\frac{V_{sz}\omega(0)}{t^2k^2(U_s')^2(U_s - c_p)}\sigma + O\left(\frac{1}{t^3}\right)\right\}\exp(\mathrm{i}\sigma)\,\mathrm{d}\sigma. \tag{B 10}$$

As the main contribution into (B 10) is due to the vicinity of $\sigma = 0$, we change the upper limit to infinity. After appropriate deformation of the integration path and term by term integration, we finally obtain for the leading term

$$\psi_{h,s} = \frac{V_{sz}\omega_0(0)}{k^3 t^2 U_s' \Delta U^2} \exp(-ikU_s t).$$

To estimate the characteristic time we derive similarly the second term

$$\psi_{h,s}^{(1)} = [M_{3,5} + M_{3,4}] \exp(-ikU_s t). \tag{B 11a}$$

$$M_{3,5} = -2i \frac{V_{sz}}{t^3 k^5 \Delta U^2} \omega(0). \tag{B 11b}$$

$$M_{3,4} = \frac{2i}{t^3 k^4 (U_s')^2 \Delta U} \{[2V_{sz} U_s'' - (U_s')^2]\omega(0) - V_{sz} U_s' \omega'(0)\}. \tag{B 11c}$$

Here the leading is term $M_{3,5}$, it gives estimation (4.12*b*). We retain the $M_{3,4}$ term with ω', because if extra vorticity is not introduced into the flow, then $\omega(0) = 0$ and the $M_{3,4}$ term becomes the leading one.

The contribution of the second endpoint can be studied similarly. The change of variables $\sigma(h) = kt(U_z - U_h)$ and intergration eventually yields

$$\psi_{h,z} \simeq \frac{\omega_0(z)}{t^2 k^2 (U_z')^2} \exp(-ikU_z t) + O(t^{-3}).$$

Calculating the second term and comparing it with the first one we obtain the characteristic time (4.12*a*) for this part of the field.

REFERENCES

Balmforth, N. J., del-Casillo-Negrete, D. & Young, W. R. 1997 Dynamics of vorticity defects in shear flows. *J. Fluid Mech.* **333**, 197–230.

Briggs, R. J., Daugherty, J. D. & Levy, R. H. 1970 Role of Landau damping in crossed-field electron and inviscid shear flow. *Phys. Fluids* **13**, 421–432.

Canuto, C., Hussaini, M. Y., Qurteroni, A. & Zang, T. A. 1987 *Spectral Methods in Fluid Dynamics*. Springer.

Case, K. M. 1960 Stability of inviscid plane Couette flow. *Phys. Fluids* **3**, 143–148.

Chandrasekhar, S. 1981 *Hydrodynamic and Hydromagnetic Stability*. Dover.

Craik, A. D. D. 1985 *Wave Interactions and Fluid Flows*. Cambridge University Press.

Dickey, L. A. 1960 Stability of plane-parallel flows of an ideal fluid. *Dokl. Akad. Nauk SSSR* **125**, 1068–1071; Eng. trans. *Sov. Phys. Doclady* **5**, 1179–1182.

Dickey, L. A. 1976 *Hydrodynamic Stability and Atmosphere Dynamics*. Gidrometeoizdat Leningrad [in Russian].

Drazin, P. G. & Reid, W. H. 1981 *Hydrodynamic Stability*. Cambridge University Press.

Dupont, R. & Caulliez, G. 1993 Caractérisation de la couche limite laminaire générée par le vent sous une interface air–eau. In *Actes du 11é Congres Français de Mecanique*, vol. 3, pp. 257–260.

Falkner, V. M. & Skan, S. W. 1931 Solutions of boundary-layer equations. *Phil. Mag.* **2**, 865–896.

Gossard, E. E. & Hooke, W. H. 1975 *Waves in the Atmosphere*. Elsevier.

Heisenberg, W. 1924 Über Stabilität und Turbulenz von Flüssigkeitsströmen. *Ann. Phys. Lpz.* **74**, 577–627.

Kelbert, M. Ya. & Sazonov, I. A. 1996 *Pulses and Other Wave Process in Fluids*. Kluwer.

Landau, L. D. 1946 On the oscillation of the electronic plasma. *J. Phys. USSR* **10**, 25.

Legras, B. & Dritschel, D. G. 1993 A comparison of the contour surgery and pseudospectral methods. *J. Comput. Phys.* **104**, 287–302.

Lin, C. C. 1955 *The Theory of Hydrodynamic Stability*. Cambridge University Press.

MASLOWE, S. A. 1981 Instabilities and the transition in shear flows. In *Hydrodynamic Instability and the Transition to Turbulence*. (ed. H. L. Swinney & J. P. Gottlub). Springer.

MILES, J. W. 1957 On the generation of surface waves by shear flows. *J. Fluid Mech.* **3**, 185–204.

MIRONOV, M. A. & SAZONOV, I. A. 1989 To the problem of discrete spectrum wave in a shear flow with sign conserved curvature of velocity profile. *Izv. Akad. Nauk. SSSR. Appl. Math. Mech.* **53**, 939–947.

PEDLEY, T. J. & STEPHANOFF, K. D. 1985 Flow along a channel with a time-dependent indentation in one wall: the generation of vorticity waves. *J. Fluid. Mech.* **160**, 337–367.

PEDLOSKY, J. 1982 *Geophysical Fluid Dynamics*. Springer.

PELINOVSKY, D. E. & SHRIRA, V. I. 1995 Collapse transformation for self-focusing solitary waves in boundary-layer type shear flows. *Phys. Lett.* A **206**, 95–202.

PULLIN, D. I. 1991 Contour dynamics method. *Ann. Rev. Fluid Mech.* **24**, 84–115.

RABINOVICH, M. I. & TRUBETSTKOV, D. I. 1991 *Oscillations and Waves in Linear and Nonlinear Systems*. Kluwer.

RAYLEIGH, LORD 1892 On the question of the stability of the flow of fluids. *Phil. Mag*. **34**, 59–70.

RAYLEIGH, LORD 1894 *Theory of Sound*, 2nd edn. Macmillan (Dover, NY, 1945, reprint of 2nd edn).

ROMANOVA, N. N. & SHRIRA, V. I. 1988 Explosive generation of surface waves by wind. *Izv. Atmos. Ocean. Phys.* **24**, 528–535.

SCHECTER, D. A., DUBIN, D. H. E, CASS, A. C., DRISCOLL, C. F., LANSKY, I. M. & O'NEIL, T. M. 2000 Inviscid damping of asymmetries on a two-dimensional vortex. *Phys. Fluids* **12**, 2397–2412.

SCHMIDT, P. J. & HENNINGSON, D. S. 2001 *Stability and Transition in Fluid Flows*. Springer.

SHRIRA, V. I. 1989 On the 'subsurface' waves in the oceanic upper mixed layer. *Dokl. Akad. Nauk. SSSR* **308**, 732–736; Eng. trans. *Trans. (Dokl.) USSR Acad. Sci. Earth Sci. Section* **308**, 276–279.

SHRIRA, V. I., IVONIN, D. V. & CAULLIEZ, G. 2002 On the laminar–turbulent transition in the wind-induced free-surface shear flows. *J. Fluid Mech.* (in preparation).

SHRIRA, V. I. & VORONOVICH, V. V. 1996 Nonlinear vorticity waves in the coastal zone. *J. Fluid Mech.* **326**, 181–203.

SMITH, F. T. 1982 On the high Reynolds number theory of laminar flows. *IMA J. Appl. Math.* **28**, 207–281.

TENNEKES, H. & LUMLEY, J. L. 1972 *A First Course in Turbulence*. MIT Press.

TREFETHEN, L. N., TREFETHEN, A. E, REDDY, S. C. & DRISCOLL, T. A. 1993 Hydrodynamic Stability Without Eigenvalues. *Science* **261**, 578–584.

VORONOVICH, A. G. & RYBAK, S. A. 1978 Explosive instability of stratified currents. *Dokl. Acad. Sci. USSR,* **239**, 1457–1460.

VORONOVICH, V. V., PELINOVSKY, D. E. & SHRIRA, V. I. 1998*b* On the internal waves – shear flow resonance in shallow water. *J. Fluid Mech.* **354**, 209–237.

VORONOVICH, V. V., SHRIRA, V. I. & STEPANYANTS, YU. A. 1998*a* Two-dimensional models for nonlinear vorticity waves in shear flows. *Stud. Appl. Maths* **100**, 1–32.